Broadband/Dual-band Metal-Mountable UHF RFID Tag Antennas: A Systematic Review. Taxonomy Analysis, Standards of Seamless RFID System Operation, Supporting IoT implementations, Recommendations and Future Directions

Fuad Erman, Slawomir Koziel, *Fellow, IEEE*, and Leifur Leifsson

***Abstract*—The employment of broadband/dual-band ultra-high frequency (UHF) radio frequency identification (RFID) tag antennas contributes to the growth of RFID technology, with many potential implications, such as the increase of international trade, and reducing costs thereof. This study presents all reported articles on RFID tags for metal objects that can work seamlessly across different countries. Moreover, it addresses all available approaches to design of wideband/dual-band metal-mountable tag antennas and showcases the techniques used to expand the tag bandwidth. The relevant works were gathered by applying a designated query '("tag antenna*" OR "RFID tag*") AND (metal*) AND ("broadband" OR "wideband" OR "dual band" OR "tri band")' in three scientific research engines. (Web of Science, IEEE Xplore, and Scopus). The final set is determined on the basis of the exclusion and inclusion criteria, revealing 38 articles. The selected papers were categorized into five groups based on the tag structure, and all techniques utilized to widen the bandwidth of each specific structure. This taxonomy attempts to provide a deeper insight into the considered topic through a comprehensive presentation. The bandwidth measurement criterion, which is 3-dB return loss (RL) bandwidth is selected due to showing an adequate reading distance on the edge of the bandwidth. In addition, the criterion clarifies the operation frequencies that facilitate the worldwide operation of the RFID technology. This paper fosters adaptation of suitable regulations to support the use of RFID systems, and researchers to design proper metal-mountable tags, which must be assessed based on operating frequencies, performance, size, cost, and compatibility with the targeted applications.**

***Index Terms*—Broadband, dual-band, metal-mountable UHF tag antenna, radio frequency identification (RFID), RFID tag standards, IoT, allocated frequencies.**

I. Introduction

RADIO frequency identification (RFID) technology deployed in ultra-high frequency (UHF) band (860-960 MHz) has been widely implemented in recent years due to its long reading distance, low cost and high reading rate. The passive RFID technology facilitates the development and progress of the Internet of Things (IoT) by making objects visible to the internet [1], [2]. This technology is extensively utilized in distribution logistics, inventory management, transportation, industries localization, and patient monitoring [3], [4]. Different factors, including antenna size, compatibility with tagged surfaces and the reading distance, play an important role in determining the performance of RFID tags [5]. The tag performance is limited by the fundamental physics-based factors implied by the tag size. Consequently, maintaining top performance whilst attempting miniaturization is challenging. However, the tag thickness is also strictly restricted because a low-profile is required in most applications. Furthermore, a simple structure implemented on inexpensive materials is crucial to minimize the fabrication cost.

The reading distance of RFID tags is influenced by the gain and radiation efficiency of the tags, as well as the threshold power of the integrated chip (IC) [6]. Furthermore, the antenna impedance is to be a complex conjugate of the IC chip impedance, which is essential to achieve maximum power transfer and the reading distance. The impedance matching can be expressed in different forms, e.g., a power transmission coefficient τ, which is an essential parameter to calculate the reading distance. The use of self-matching approaches is preferable over discrete components due to fabrication cost. Thus, the capability to modify the antenna geometry is important to obtain a desired input impedance and radiation properties. Different types of computational electromagnetic software packages have been employed to facilitate the development and optimization of antenna geometry, e.g., CST Microwave Studio and Ansoft HFSS [7]–[9]. Obtaining RFID

This paper has been submitted to the IEEE IoT Journal on Sep 28th, 2022. This work was supported in part by the Icelandic Centre for Research (Rannsóknamiðstöð Íslands-RANNIS) Grant 174573, and by the National Science Centre of Poland Grant 2018/31/B/ST7/02369. *(Corresponding author: Fuad Erman).*

Fuad Erman is with Engineering Optimization & Modeling Center, Reykjavik University, 102 Reykjavik, Iceland and with College of Telecommunications and Information Technology, Nablus University for Vocational & Technical Education, 110, Ramallah, State of Palestine (e-mail: fuadnaime@ru.is; fuadnae@gmail.com).

Slawomir Koziel is with Engineering Optimization & Modeling Center, Reykjavik University, 102 Reykjavik, Iceland and with Faculty of Electronics, Telecommunications and Informatics, Gdansk University of Technology, 80-233 Gdansk, Poland (e-mail: koziel@ru.is).

Leifur Leifsson is with School of Aeronautics and Astronautics, Purdue University, West Lafayette, IN 47907-2045, USA (e-mail: leifur@purdue.edu).

tags featuring excellent performance whilst mountable onto different surfaces, especially metal objects, is a pressing concern because the surface where the RFID tag is placed can affect its operation [10]. Radiated electric fields deteriorate due to the cancellation between the radiating current and its image counterpart. This effect disturbs the reading range, the input impedance and the radiation efficiency but it is dependent on the shape and the size of the metal structures. The main limitations in designing UHF RFID tags lie in the size-performance ratio because the existence of conductive surfaces in a proximity is a notable obstacle.

A broadband operation is desirable because allows the tag to work over a wide range of frequencies and to overcome frequency fluctuation issues due to fabrication defects. In addition, broadband tags work seamlessly in different countries worldwide because they cover all adopted frequencies based on the specific regulations of the country. The bandwidth specification defines the matching level of impedance between the IC chip and the RFID tag, wherein researchers adopted half-power bandwidth (3-dB return loss *RL*, bandwidth) for RFID tags to measure its bandwidth over UHF frequencies [11]. This criterion includes an acceptable reading range on the bandwidth edge compared with that at the resonant frequency.

Well-designed UHF tag antennas exhibit an operation bandwidth that offers seamless work worldwide. In addition, compatibility with various surfaces regardless of their size and shape is desired yet difficult to achieve. This review presents the literature works categorized into two levels, wherein classification is based on tag structure and all techniques of widening the tag bandwidth are arranged for each specific structure in the sub-categories. The literature works were gathered using a specific query that was applied in scientific research engines, and the final set of 38 articles was reported in this study. The standards of wideband/dual-band tag operations are introduced in a separate section, revealing the necessary allocated frequencies to design a tag with seamless operation worldwide and presenting the measurement criterion of the tag bandwidths. The RFID technology has witnessed rapid growth and widespread applications; thus, the governments should define regulations to support the efficient operation of the RFID technology worldwide. In a related vein, the researchers are encouraged to design RFID tags that are compatible with the proposed applications with the emphasis on low-profile miniature structures and the absence of cross-layered construction.

II. Methods

A systematic review of the literature in the field of UHF RFID tags was executed in accordance with the chosen items for reporting a review and meta-analyses [12]. This approach is used to identify the literature on a defined topic. Accordingly, distinct steps are followed to apply a systematic procedure for the determination, selection, and careful evaluation of the related literature to gather a compendium of the reported studies. Such a procedure is advantageous over conventional approaches. In particular, it allows the researchers to integrate the reported works into a clear, precise, and easily reproducible pattern. The systematic review procedure comprises different stages, including the determination of the research topics, search methods, and research selection standards; the extraction of the required information and data synthesis.

A. Research Topic

The defined topic of this study is wideband and dual-band UHF RFID tag antennas for metallic applications. In this systematic review, a wideband/dual-band tag antenna is defined as an RFID tag that can work effectively over the frequency range of 865-928 MHz or covers the Lower European and North American bands, respectively. This feature is a requirement for the designed tags to work seamlessly worldwide, and to be in compliance with the regulations of different countries in terms of the operating frequency range. The target articles were combined by applying a specific query in the scientific research engines that covered the defined topic. Furthermore, all recently developed approaches of designing RFID tag and expanding the bandwidth, operation standards, and recommendations and future directions were reported.

B. Source and Search Strategy

The literature search was performed on 15 July 2022 in recognized scientific search engines as follows:

- IEEE Xplore Library, which provides high-quality research works and the most highly cited articles in the engineering and technology fields.
- Web of Science (WoS) platform, which covers journals in various disciplines including scientific, social science, and medical journals.
- Scopus, which is the largest database of academic research articles.

These databases were selected because of indexing high-impact academic journals that are adequate for carrying out this systematic review. The search strategy was performed by using three groups of keywords and Boolean operators (i.e., OR, AND) that are utilized in the search of the scientific articles. The assigned query was used to determine the most related articles to the topic of this review in the aforementioned research engines. The setting of the search engines was limited to English language, whereas the publication types included journals and conferences. However, the time period was not specified. Table I shows the setting of the applied query.

C. Study Selection and Criteria

The inclusion and exclusion criteria were restricted on the basis of the assigned query that was implemented in the scientific research engines to gather the compatible articles within the research scope (broadband/dual-band UHF RFID tag antenna for metallic applications). The engines were set as shown in Table I. After implementing the designed query, various stages of screening and filtering were performed. A MS Excel file containing the title, abstract, keywords, journal name, year of publication, authors' names and affiliations, and publication types was exported from all utilized engines (IEEE Xplore, WoS, and Scopus). First, all irrelevant documents were discarded. In addition, all the duplicate articles were identified

TABLE I

SETTING OF THE APPLIED QUERY IN SEARCH ENGINES

Digital Library	IEEE Xplore	WoS	Scopus
Publication Periods	All range	All range	All range
Language	English	English	English
Publication Types	Journals and Conferences	Journals and Conferences	Journals and Conferences
Search Domain	Metadata	TS = Topic	TITLE-ABS-KEY
Date of Search	Jul 2022	Jul 2022	Jul 2022

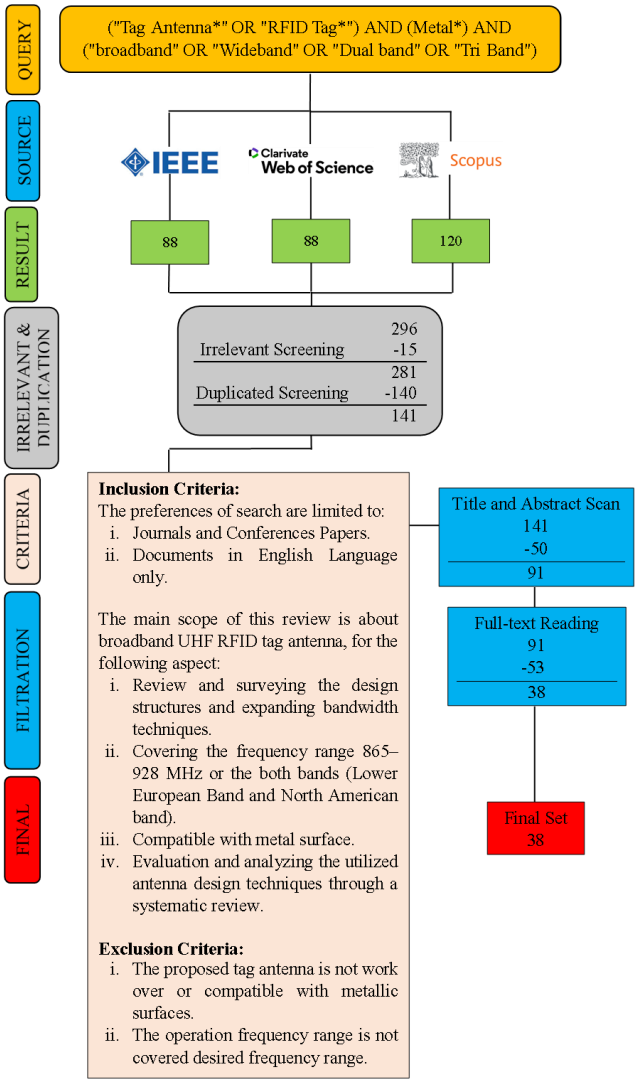

Fig. 1. Flowchart of systematic review procedure stages.

and removed. In the second stage, titles and abstracts were screened to discard the irrelevant articles that were exported. At this stage, the remaining articles should match the eligibility criteria of this review. The full texts of the remaining articles were viewed for proper selection. In the screening and filtering stages, all articles that did not match the design specifications in terms of the desired bandwidth, were excluded, whereas the articles that accurately matched the selection criteria were considered.

D. Statistical Results and Extraction of Required Information

Three groups of keywords were linked by using Boolean operators (‘AND’ and ‘OR’) to cover the research scope. The query entered in the advance research box of the scientific research engines was ("tag antenna*" OR "RFID tag*") AND (metal*) AND ("broadband" OR "wideband" OR "dual band" OR "tri band") as seen in Fig. 1. The performed research yielded 296 articles comprising 88 articles from WoS, 88 articles from IEEE Xplore and 120 articles from Scopus. In the beginning, all irrelevant articles, including 15 conference reviews, were removed. Then, three stages of filtering and screening were performed to identify the articles for inclusion in this study. The first stage of filtering involved discarding duplicated articles, i.e. 140 articles out of 281. After screening the titles and abstracts of the remaining 141 articles, another 50 articles were further excluded. Therefore, 91 articles were included. At the next stage, 53 articles were discarded while doing a full-text review. A total of 38 articles (journal and conference papers) were selected and considered as the backbone of the reviewed topic. The selected articles were grouped in accordance with different categories. All of the tag designs, and broaden bandwidth approaches were extracted, which provide a good overview of the topic, and facilitates shaping the final presentation of this systematic study. Furthermore, additional data were extracted for insertion into the Excel file. These data included read range, realized gain, achieved bandwidth, materials, permitted radiated power of reader, tag size, and mounted IC chip specifications. These data were summarized, described, and tabulated to help presenting this study in an appropriate manner.

III. STANDARDS OF SEAMLESS RFID SYSTEM OPERATION

Standards are understood as the rules applied by different bodies to structures in any industry or commercial activity; they are essential in expanding the globalized economy and reducing expenses. The global system of standards gives a framework that permits information, products and services to move securely and efficiently for the benefit of people’s lives. These standards allow different parties to work together efficiently, thus enabling new services and smooth global communications [13]. This section presents the standards of a design tag antenna with a wideband operation. The allocated frequencies are determined after studying national regulations in each country. Furthermore, this section exactly defines the specific frequencies where a wideband/dual-band RFID tag steadily operates and the measurement criterion for the tag bandwidth. Attempting to define these standards supports the seamless works of the RFID technology worldwide.

A. Allocated Frequencies

The UHF band covers the frequency range from 300 *MHz* to 1 *GHz*, wherein the UHF RFID system is allocated over a particular range of frequencies (860– 960 *MHz*). The components of RFID systems (tags, antenna, and the reader) should be in compliance with regulations of respective countries in terms of the operating frequency and maximum effective isotropic radiated power *EIRP*, or effective radiated

power *ERP*. National regulations determine the UHF RFID frequency ranges that differ between countries. These frequency ranges are recognized as industrial, scientific, and medical (ISM) bands. The UHF RFID technology uses two major frequency bands: the North American band (902–928 *MHz*, 4 *watts EIRP*) and the Lower European band (865–868 *MHz*, 2 *watts ERP*). The latter is called the Lower European band due to the decision of Commission Implementing Decision (EU) on 11 October 2018 on the allocation of the Upper European band (915–921 *MHz*, 4 *watts ERP*). In addition to the aforementioned bands, researchers previously mentioned the existence of the Japan bands (952–956.4 and 952-957.6 *MHz*, 4 *watts EIRP*). However, this band was effective only until the end of July 2012. At present, Japan band falls within the North American band where its current range is 916.7–920.9 *MHz* (4 watts EIRP). This detail is based on the last updated version from the Global System of Standards (GS1) [14]. A few countries have taken on single or multiple ranges in the ISM standard outside the Lower European and the North American bands. Most GS1 members (81 countries), except for Algeria, Brunei Darussalam and New Zealand, have adopted frequency ranges within the Lower European band, the North American band or in both bands. The National Frequency Agency in Algeria also adopted the ranges of 870–876, 880–885, 915–921 and 925–926 *MHz*. In Brunei Darussalam, the Authority for Info-communications Technology Industry adopted the frequency ranges of 866–869 and 923–925 *MHz*. Meanwhile, the Ministry of Economic Development in New Zealand adopted the two frequency ranges of 864-868 and 920–928 *MHz*. Hence, RFID tags, which are designed to operate over the frequencies of 865–928 *MHz* or cover the Lower European and the North American bands are regarded as broadband/dual-band UHF RFID tag antennas that work seamlessly across different countries.

B. Bandwidth Criteria

The *RL* response of the tag antenna is a vital performance indicator that is measured after performing simulation and fabricating prototype for verification. Achieving an excellent *RL* response means obtaining an ideal impedance matching with an IC chip, in which a maximum power transfer is received by the IC chip. Notably, an ideal *RL* response does not indicate good radiation properties; thus, verifying the radiation performance is also crucial. The performance of the tag can be evaluated on the basis of its radiation efficiency and gain. In addition, obtaining ideal impedance matching to ensure perfect power transfer between the IC chip and antenna, which is reflected in the read range of designed tag, is essential [6].

RL can be computed using the power reflection coefficient, $|S|^2$ as

$$RL\ (dB) = -10\log|S|^2, \tag{1}$$

where $|S|^2$ is given by

$$|S|^2 = \left|\frac{Z_{Ant} - Z_{Chip}^*}{Z_{Ant} + Z_{Chip}}\right|^2, \tag{2}$$

where Z_{Ant} and Z_{Chip} are the input impedance of antenna and IC chip respectively.

As expected, achieving the matching condition as indicated in (2) means that the value of the power reflection coefficient is equal to zero ($|S|^2 = 0$) [15].

$$R_{Ant} = R_{Chip}\ and\ X_{Ant} = -X_{Chip}. \tag{3}$$

The power transmission coefficient τ can be obtained from $|S|^2$ as

$$\tau = 1 - |S|^2. \tag{4}$$

A relationship is observed between the measured *RL* and the value of τ based on Equations (1) and (4). In particular, *RL* determines the value of τ over the desired frequency range. Ideal matching with IC chip means $|S|^2 = 0$ and $\tau = 1$. Consequently, the tag reading range r, is equal to the maximum possible value, which can be computed as

$$r = \frac{\lambda}{4\pi}\sqrt{\frac{P_{EIRP}G_a\tau}{P_{th}}}. \tag{5}$$

where λ is the wavelength, P_{EIRP} is the allowed output power of the RFID reader according to country regulations, P_{th} refers to the minimum required power to activate IC chip, and G_a is the tag's gain.

Achieving perfect matching ($\tau = 1$) results in obtaining the maximum possible reading range

$$r_{max} = \frac{\lambda}{4\pi}\sqrt{\frac{P_{EIRP}G_a}{P_{th}}}, \tag{6}$$

The impedance matching of the RFID tag is defined using half-power bandwidth ($RL \geq 3$), wherein the tag bandwidth can be measured [11]. The performance of the RFID tag can be also assessed considering the read range at the edge of the 3-dB *RL* bandwidth r_{3-dB}. It can be evaluated by considering the relative value of r_{3-dB} with respect to r_{max}. It can be computed as follows. The value of power reflection coefficient at the edge of 3-dB *RL* bandwidth, $|S|^2_{3-dB}$ can be obtained from (1) with $RL = 3\ dB$. τ_{3-dB} is then obtained by subtituting $|S|^2_{3-dB}$ to (4). Consequently, the value of r_{3-dB} is equal to 70.6% r_{max}:

$$|S|^2_{3-dB} = 10^{-RL(dB)/10} = 10^{-3/10} = 0.5012$$

$|S|^2_{3-dB}$ is substituted in (4) to compute τ_{3-dB},

$$\tau_{3-dB} = 1 - |S|^2_{3-dB} = 1 - 0.5011 = 0.4988$$

Finally, r_{3-dB} is expressed as the fraction of r_{max} as follows

$$r_{3-dB} = \frac{\lambda}{4\pi}\sqrt{\frac{P_{EIRP}G_a\tau_{3-dB}}{P_{th}}} = \frac{\lambda}{4\pi}\sqrt{\frac{P_{EIRP}G_a}{P_{th}}} \times \sqrt{\tau_{3-dB}}$$

$$r_{3-dB} = 70.6\%\ r_{max}.$$

The computed r_{3-dB} fulfilled the reading range requirement over the operation bandwidth. Thus, 3-dB *RL* bandwidth is suitable to measure the bandwidth of the RFID tags and could be used as criterion to evaluate its bandwidth. The performance of the tag within the 3-dB *RL* bandwidth is considered acceptable.

IV. TAXONOMY

The target articles, which are combined by applying the designed query and used to define the topic, form a comprehensive presentation of this review. The paper focuses on the techniques used to design UHF RFID tags and all

TABLE II

COMPARISON OF WIDEBAND/DUAL-BAND METAL MOUNTABLE UHF RFID TAGS FOR METALLIC OBJECTS

Ref	Size (mm^3)	P_{EIRP} (Watt)	P_{th} (dBm)	G_r (dB)	r (m)	BW (MHz)	Substrate
[17]	$73 \times 30 \times 1.6$	3.2	-15	Gain -5^{S}	$3^{C/LEu}$ $2.6^{C/NA}$ $4.3^{C/JP}$	$(838-970)^{S/HPRC}$	FR4
[18]	$73 \times 50 \times 2$	4	-14	-	5.13^{C}	$657-1250^{S/10RL}$	FR4
[19]	$87 \times 45 \times 1.6$	-	-18	Gain -7.2^{S}	-	$159^{S/3RL}$ $155^{M/3RL}$	FR4
[20]	$130 \times 63 \times 1.6$	3.3^{LEu} 4^{NA}	-18	Gain $-11.5^{S/LEu}$ $-10.56^{S/NA}$ $-12.06^{S/JP}$	$3.33^{C/LEu}$ $3.61^{C/NA}$ $2.8^{C/JP}$	$113^{S/6RL}$ $117^{M/6RL}$	FR4
[21]	$D = 33 \times 1.6$	3.3^{LEu} 4^{NA}	-16.7	Gain -6.9^{S}	$4.5^{C/NA}$	$820-980^{S/10RL}$	FR4
[22]	$114 \times 50 \times 1.5$	4	-18	Gain $-0.6^{S/NA}$	$8.1^{M/NA}$	$66^{S/3RL}$ $84^{M/3RL}$	Teflon
[23]	$26 \times 11 \times 1.6$	-	-17.4	-	-	$800-940^{S/10RL}$	FR4
[24]	$91 \times 44 \times 1.6$	-	-13	-	-	$836-984^{S/3RL}$ $856-1000^{M/3RL}$	FR4
[25]	$139 \times 32 \times 1.6$	3.3^{LEu}	-20	0.94^{S}	$17.6^{C/LEu}$ $16.8^{C/NA}$	-	FR4
	$88 \times 32 \times 1.6$			-7.8^{S}	$6.4^{C/LEu}$ $6.1^{C/NA}$		
	$88 \times 32 \times 3.2$			-4.4^{S}	$9.6^{C/LEu}$ $9^{C/NA}$		
[26]	$85 \times 40 \times 3.2$	3.3^{LEu} 4^{NA}	-20	-	$11^{C/LEu}$ $9.7^{C/NA}$	-	FR4
	$85 \times 40 \times 1.6$				$4^{C/LEu}$ $3.7^{C/NA}$		
[27]	$137 \times 32 \times 1.575$	4	-14	-	5^{M}	$840-960^{S/3RL}$	Rogers RT5880
[28]	$85.5 \times 73 \times 1.6$	-	-13	Gain $-1^{S/LEu}$ $-6^{S/NA}$	$6.5^{C/LEu}$ $4.5^{C/NA}$	$823-971^{S/HPRC}$	FR4
[29]	$100 \times 100 \times 1.6$	3.98	-17.4	Gain -7.9^{S}	4.67^{C} 4.36^{M}	$880-940^{S/HPRC}$ $857-983^{M/HPRC}$	FR4
[30]	$35 \times 15 \times 3.54$	-	-6.9	Gain $0.13^{S/LEu}$ $0.7^{S/NA}$	$3^{M/LEu}$ $2.9^{M/NA}$	-	Rogers RT6010.2LM
[31]	$90 \times 30 \times 0.55$	0.25	-17.4	-	$3.5^{M/LEu}$ $3.6^{M/NA}$	$847-877^{SFPA/20RL}$ $877-930^{SSPA/20RL}$	Polypropylene
[32]	$50 \times 98 \times 1.6$	4	-13	Gain $-3.68^{S/LEu}$ $-4^{S/NA}$	$4.8^{S/LEu}$ $4.9^{S/NA}$	$835-966^{S/3RL}$	FR4
[33]	$76 \times 60 \times 1.6$	1	-14	-1.5^{S}	4.2^{M}	$850-940^{S/VSWR}$	FR4
	$84 \times 26 \times 1.6$		-18	-3^{S}	4^{M}	$850-950^{S/VSWR}$	
[34]	$65 \times 65 \times 2$	1	-14	-	3.5^{M}	$840-955^{S/3RL}$ $855-980^{M/3RL}$	FR4
[35]	$50 \times 96 \times 2$	3.3^{LEu} 4^{NA}	-13	-	$4.5^{M/LEu}$ $4.3^{M/NA}$	$837-975^{S/3RL}$ $842-975^{M/3RL}$	FR4

Ref	Size (mm^3)	P_{EIRP} (Watt)	P_{th} (dBm)	G_r (dB)	r (m)	BW (MHz)	Substrate
[36]	$75 \times 42 \times 2$	-	-18	$2.38^{M/LEu}$ $-1.18^{S/NA}$ $-1.83^{M/NA}$	-	$790-1040^{S/10RL}$ $770-1025^{S/10RL}$	FR4
[37]	$26.5 \times 26.5 \times 3$	4	-18	-	$11^{C/Eu}$ $13.5^{C/NA}$ $10^{M/Eu}$ $12^{M/NA}$	$5^{M/3RL/Eu}$ $8^{M/3RL/NA}$	Ceramic
[38]	$80 \times 31 \times 0.5$	4	-18	Gain -5.86^{S}	5.2^{M}	$856-953^{S/10RL}$	PET
[39]	$37 \times 7 \times 3.2$	3.28	-18	-8.8^{S}	2^{M}	-	Rogers 4003
[40]	$68 \times 68 \times 1.6$	3.98	-17.4	Gain -10.2^{S}	3.7^{S} 3.45^{M}	$790-971^{M/10PRC}$	FR4
[41]	$20 \times 35 \times 1.6$	-	-17.4	-	-	$800-877^{S/10RL}$ $904-926^{S/10RL}$ $943-975^{S/10RL}$	FR4
[42]	$85 \times 50 \times 1.9$	0.5	-	Gain $-2.8^{M/LEu}$ $-9.7^{M/NA}$	$1.7^{M/LEu}$	-	Rogers TMM3
[43]	$D = 30 \times 3.4$	-	-14	-	3.2^{M}	$840-973^{S/3RL}$ $845-960^{M/3RL}$	FR4 + Air gap + Ground Plane
[44]	$D = 29.5 \times 3.6$	-	-14	-	3.8^{M}	$833-968^{S/3RL}$ $848-963^{M/3RL}$	FR4 + Air gap + Ground Plane
[45]	$70 \times 30 \times 3.6$	4	-14	-	5.2^{M}	$853-975^{S/3RL}$ $850-962^{M/3RL}$	FR4 + Air gap+ Ground Plane
[46]	$60 \times 60 \times 6.27$	3.3^{LEu} 4^{NA}	-	-	$14^{M/Eu}$ $11^{M/NA}$	-	Rogers RO30100 + Air gap+ Ground Plane
[47]	$95 \times 49.5 \times 4.6$	-	-10	-	$8.8^{C/Eu}$ $8^{C/NA}$	$858-878^{S/3RL}$ $898-929^{S/3RL}$	FR4 + Foam + Ground Plane
[48]	$106 \times 44 \times 4.6$	3.3^{LEu} 4^{NA}	-10	-	$3.4^{C/Eu}$ $4.1^{C/NA}$ 2.9^{M}	$842-950^{S/3RL}$ $842-960^{M/3RL}$	FR4 + Foam + + Ground Plane
[49]	$47 \times 21 \times 2.36$	4	-20.85	$-8--11^{S}$ -8^{M}	$5.5^{M/LEu}$ $5.5^{M/NA}$	$854-945^{S/3RL}$	Rogers RT6002 + Wrapped FR4 with Polyimide film
[50]	$75 \times 20 \times 3$	-	-17.4	3.3	3.8^{M}	$795-992^{S/10RL}$	FR4 + Rogers RT4003 covered by metal strap
[51]	$104 \times 31 \times 7.6$	3.3^{LEu} 4^{NA}	-18.5	$-0.91^{M/LEu}$ $0.6^{M/NA}$ $-6.9^{M/JP}$	$11.8^{M/LEu}$ $14.6^{M/NA}$ $6^{M/JP}$	-	2 FR4s separated by Air gap
[52]	$56 \times 26 \times 3.2$	4	-15	$-9.2^{M/LEu}$ $-4.3^{M/NA}$ $-5.5^{M/JP}$	3.1^{S} 3.5^{M}	$863-965^{M/3RL}$ $840-980^{M/3RL}$	2 FR4s
[53]	$84 \times 42 \times 14$	-	-18	Gain 2.18^{S}	-	$810-930^{S/10RL}$	FR4 + Air gap + substrate + foam
[54]	$190 \times 190 \times 15.8$	-	-15	-	$5.5^{C/Eu}$ $6.9^{C/NA}$ $2.8^{M/Eu}$ $6^{M/NA}$	$840-853^{S/10RL}$ $916-925^{S/10RL}$ $825-945^{S/3RL}$	FR4 + Air gap + Reflector

[S] Simulation Value
[M] Measurement Value
[C] Theoretical Value
[LEu] Lower European Band
[NA] North American Band
[C/LEu] Theoretical Value in Lower European Band
[C/NA] Theoretical Value in North American Band
[C/JP] Theoretical Value in Japan Band
[M/LEu] Measurement Value in Lower European Band
[M/NA] Measurement Value in North American Band
[M/JP] Measurement Value in Japan Band
[S/LEu] Simulation Value in Lower European Band
[S/NA] Simulation Value in North American Band
[S/JP] Simulation Value in Japan Band
[S/HPRC] Simulation Value of Half-Power Reflection Coefficient Bandwidth
[M/HPRC] Measurement Value of Half-Power Reflection Coefficient Bandwidth
[M/10PRC] Measurement Value of 10-dB Power Reflection Coefficient Bandwidth
[S/3RL] Simulation Value of 3-dB *RL* Bandwidth
[M/3RL] Measurement Value of 3-dB *RL* Bandwidth
[M/3RL/LEu] Measurement Value of 3-dB *RL* Bandwidth in Lower European Band
[M/3RL/NA] Measurement Value of 3-dB *RL* Bandwidth in North American Band
[S/6RL] Simulation Value of 6-dB *RL* Bandwidth
[M/6RL] Measurement Value of 6-dB *RL* Bandwidth
[S/10RL] Simulation Value of 10-dB *RL* Bandwidth
[SFPA/20RL] Simulation Value of First Patch Array 20-dB *RL* Bandwidth
[SSPA/20RL] Simulation Value of Second Patch Array 20-dB *RL* Bandwidth
[S/VSWR] Simulation Value of Voltage Standing Wave Ratio < 3

reported approaches to expand their bandwidth. Notably, the considered studies are limited to designs that can be able mounted onto metal surfaces and operate over the frequencies of 865–928 MHz or coverer the Lower European and the North American bands. The taxonomy was performed on two levels. In the first level, the selected studies are split into five categories based on the tag structure. For each specific structure, all the approaches employed to broaden the tag bandwidth are then introduced as sub-categories. Furthermore, all reported RFID tags in this section are summarized in Table II, which includes the tag size, permitted radiated power of the reader, realized gain, reading range, IC chip threshold power, and bandwidth. This section presents the applied taxonomy of the titled topic to provide a deeper sight into the reported literature.

A. Single-Layer without Cross-Layered Construction:

The tag antennas should be inexpensive, its structure must be simple, which is a prerequisite for mass production. It should also exhibit appropriate performance. These are essential factors for a passive RFID system. The structures reported in this sub-section do not involve cross-layered construction, are low-profile, allow easy fabrication, and work properly when mounted onto metallic surfaces. To enable this, a metallic plane is coated on the back of a substrate to uphold an excellent performance whilst the tag is placed on a metallic surface. In addition, the metallic structure must be identified as a ground plane and improve the tag operation as it acts as a reflector [16]. The literature extracted on the basis of the query discussed earlier reports various low-profile single-layer structures without cross-layered construction to design broadband/dual-band UHF RFID tag antennas for metallic applications. The structure and the employed approaches to expand tag bandwidth will be discussed in the following sub-sections.

1. Parasitic Elements:

Utilization of the parasitic elements to expand the operation bandwidth of RFID tags has been considered in numerous works. Technically, the parasitic elements are effectively used to excite new resonant frequencies near the fundamental mode. This excitation results in broadening the tag bandwidth; however, this approach suffers from a large size of the antenna. In [17]–[20], the tag structure comprises rectangular or triangular feeding loop inductively coupled feed parasitic patches in different shapes, such as meandered, rectangular, and U- or C-shaped patches. The tag impedance is observed at the input terminal of the feed loop as given in [55]:

$$Z_{in} = Z_{loop} + \frac{(2\pi fM)^2}{Z_{ant}}, \tag{7}$$

where Z_{ant} is the antenna impedance of parasitic elements, $Z_{loop} = j2\pi fL_{loop}$ is the impedance of feeding loop, M is the mutual coupling determined by loop dimensions and coupling distance and f is the operating frequency. At the input terminal, the resistance and reactance can be respectively computed as follows:

$$R_{in} = (2\pi fM)^2 / R_{ant} \tag{8}$$

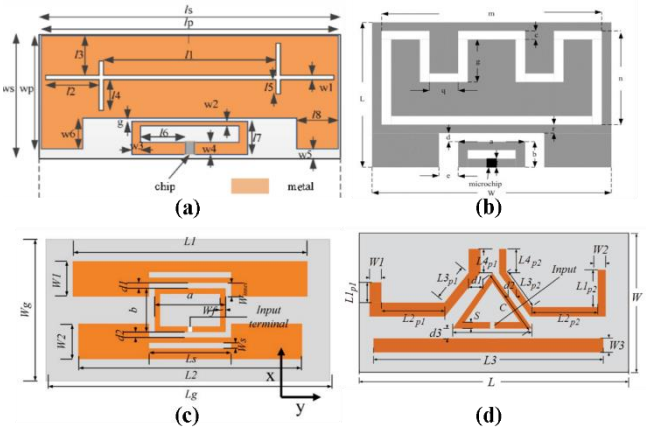

Fig. 2. Feeding loops for: (a) U-shaped patch [17] (b) two radiating patches [18], (c) two C-shaped patches [19], and (d) coplanar multi-resonator configuration [20].

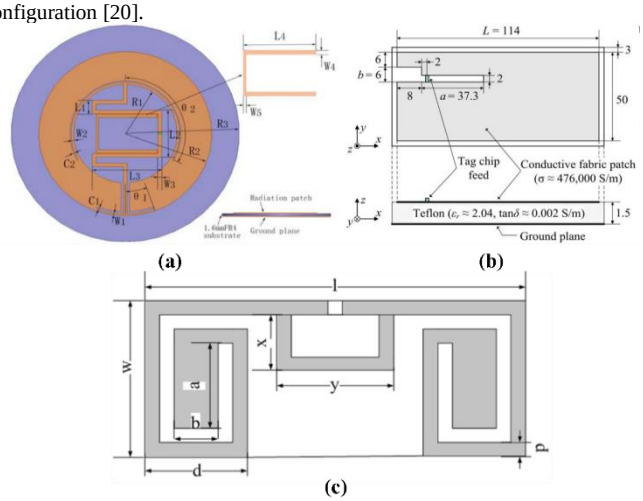

Fig. 3. RFID tags based on module matching mode **(a)** a hybrid microstrip and coplanar waveguide structure [21] **(b)** a rectangular patch with longitudinal two step staircase slit [22] **(c)** T-matching network and modified dipole connected with symmetrical capacitive tip loadings [23].

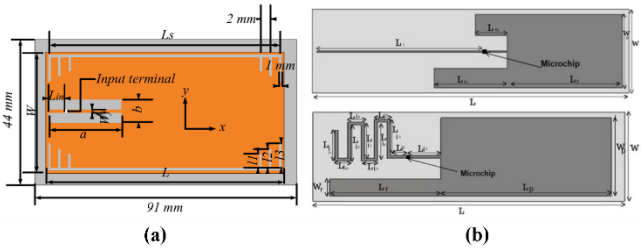

Fig. 4.(a) Rectangular patch with inset-feed lines with embedded key-shaped slots [24] **(b)** modified patch loaded with open or meandered stub [25], [26].

$$X_{in} = 2\pi fL_{loop} \tag{9}$$

Equations (8) and (9) reveal that the resistance can be determined by adjusting M whilst the reactance is merely identified by the loop inductance.

In [17], the tag antenna comprises a rectangular feed loop that is an inductively coupled feed U-shaped patch. The operation bandwidth of this antenna is expanded by embedding orthogonal symmetric slots into the horizontal slot on the radiating patch as shown in Figure 2(a). This expansion entails two excited resonant frequencies adjacent to the fundamental mode. The excited resonant frequencies can be optimized by

adjusting the length of the odd symmetrical slots. In [18], the structure is similar to the previous design (a rectangular feed loop and U-shaped patch) but a slot is applied, forming two radiating patches as shown in Figure 2(b). The structure realizes two resonant frequencies, resulting in a wideband tag. In [19], the reported tag comprises a rectangular feed loop and two C-shaped patches as exhibited in Figure 2(c). The two radiating patches are defected from one side to form two C-shaped patches to enable size reduction. Wideband operation is ensured by generating two resonant frequencies close to each other, and two C-shaped patches are used to excite both frequencies. The two embedded horizontal slots are adjusted to control the two excited resonant frequencies. In [20], three different patches are inductively coupled and feed by a triangular feed loop as shown in Figure 2(d). Wideband performance is obtained due to coplanar multi-resonator configuration that excites three resonant frequencies adjacent to the fundamental mode.

2. Module Matching Mode:

Accomplishing conjugate matching covering a wide frequency range is challenging due to the change in the resistance and reactance values of IC chips over different frequencies. Thus, the module matching mode was investigated considering the power transmission coefficient (impedance matching coefficient τ) characteristics of RFID tag to solve the aforementioned issue. Antenna structures are adjusted by embedding slits, slots or parasitic elements to ensure that the impedance is consistent with the IC chip impedance over a wide range of frequencies. The tag designed this way shows a proper performance over all desired frequency ranges, by effectively eliminating impedance mismatch [56]. The module matching mode is an ideal approach to achieve broadband RFID tags. The maximum power transfer between antennas and IC chips indicates the realization of ideal impedance matching. This transfer defines the degree of impedance matching over a range of frequencies and is computed as

$$\tau = 4\,R_{IC}R_{ant}/|Z_{IC} + Z_{ant}|^2, \quad 0 < \tau < 1 \qquad (10)$$

where Z_{IC} and Z_{ant} are the input impedance of the mounted chip and tag antenna, respectively. R_{IC} is the IC chip resistance and R_{ant} is the resistance of the tag antenna.

In [21], a tag structure was proposed based on a ring with known inner and outer diameters, wherein asymmetric arc transmission feedlines formed by two arc-shaped slots are aligned inside and outside the ring edge as shown in Figure 3(a). The transmission feedline lengthens to reduce the antenna size. The dimension of the transmission feedlines is modified to obtain an impedance module matching in a broadband range. A parasitic U-shaped patch positioned in the middle of transmission lines features a tunable dimension to accurately adjust the impedance (real and imaginary parts). In [22], a rectangular patch without cross-layered construction is proposed, where a longitudinal two-step staircase slit was embedded. The outer part of the slit is wider than that of the inner step and the IC chip mounted between the two steps. The lower side of both steps are aligned to each other as seen in Figure 3(b). The antenna impedance was controlled by adjusting the dimensions of the slit, specifically, the width of the outer step, and the length of the inner step. Such an adjustment results in a tag featuring a broad bandwidth due to a wide impedance match between the antenna and the IC chip. In [23], a miniature tag has been proposed that comprises a T-matching network and a modified dipole loaded with two symmetric capacitive tip loadings as shown in Figure 3(c). The T-matching network acts as an inductor, L_t whilst the capacitive tip loading performs as C_t. The tag resonant frequency, f_c relays on the value of L_t and C_t, which can be computed using the following formula,

$$f_c = 1/\left(2\pi\sqrt{L_t C_t}\right) \qquad (11)$$

The value of L_t and C_t depends on the dimensions of the short-circuit stub of T-matching network and the width of capacitive tip loading, respectively. A compact size with high inductance is accomplished by loading the end of the modified dipole with capacitive tip loadings. The tag bandwidth is broadened due to the adjustment of the T-matching network.

3. Adjusting/Defecting Main Radiating Body

Molding the structure or embedding slots on the main radiating body could excite a new resonant frequency adjacent to the fundamental mode, which gives the capability to render a wideband performance to the tag antenna. This approach can reduce the designed tag size as opposed to the employment of parasitic elements as discussed in the first subsection.

In [24], the rectangular patch was defected near the radiating edge, with a slot and the feedlines inset inside the slot to connect the IC chip directly, as shown in Figure 4(a). Notably, a pair of symmetrical key-shaped slots aligned to the non-radiating edges of the main radiated patch. The embedded slots excite a second resonant frequency near the main mode, which broadens the tag bandwidth. However, embedding the slots is detrimental to the gain/radiation efficiency of the tag [57]. [25], [26] presented the structured following the same concept and proposed tags with a dual-band performance. The tag reported in [25] comprises a modified patch loaded with open stub as shown in Figure 4(b). The chip is mounted between the radiating patch and the open stub. A miniaturized prototype, which consists of a modified patch loaded with a meandered stub has been shown in Figure 4(b). Both resonant frequencies can be adjusted by altering the dimensions of a modified patch (narrow parts of the modified patches) and the open stubs. The performance of the miniaturized tag was improved by utilizing a thick substrate with a thickness of 3.2 mm.

B. Single-Layer with Cross-Layered Construction:

Different solutions have been presented to overcome the presence of metallic surfaces nearby or attached to the tag. The backside of the tag is fully laminated with copper to maintain its good performance whilst mounted onto metallic structures. Furthermore, the radiating elements are grounded to provide extra immunity to the conductive objects. The structure should comply with the following design requirements: low-profile structure, adequate reading range, compact size, inexpensive fabrication, and perfect impedance matching to assure maximum power transfer between the IC chip and the antenna. In this subsection, the exhibited studies were chosen from the

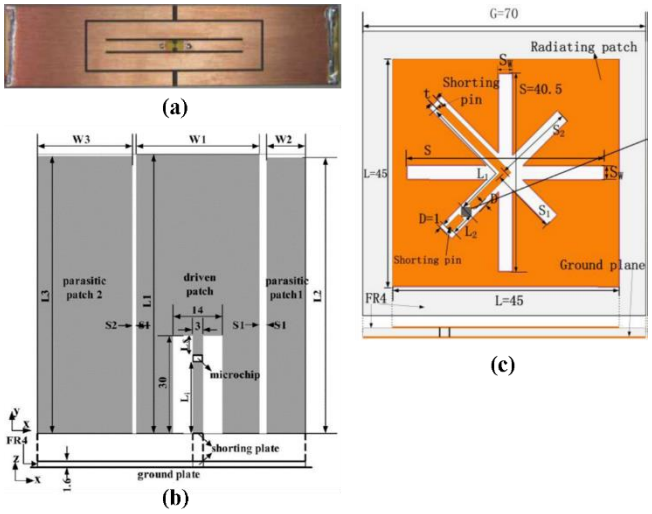

Fig. 5. (a) A loop with inset feedline inductively coupled feed the shorted patches [27] **(b)** the driven patch with inset feedline grounded capacitive-coupled the additional parasitic patches [28] **(c)** a grooved patch with embedded grounded feed network [29].

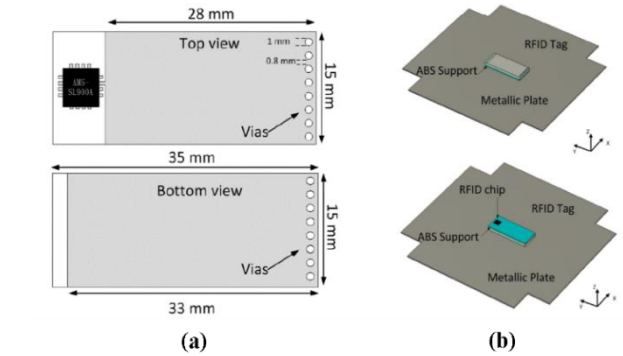

Fig. 6. (a) The tag antenna with uneven length of parallel laminated copper plane [30] **(b)** flipping tag on metallic surfaces to change the operating bandwidth (Lower European or North American bands) [30].

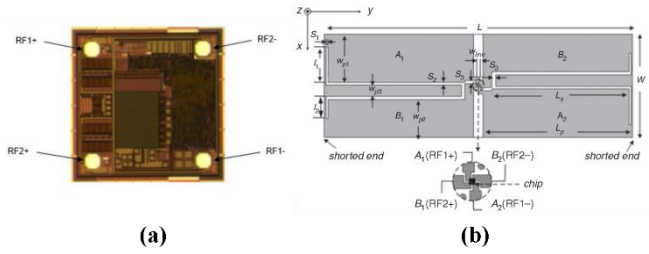

Fig. 7.(a) Impinj Monza 4 IC chip configuration [58] **(b)** tag antenna comprises two patch arrays, which have a cross-connection with Monza 4 IC chip [31].

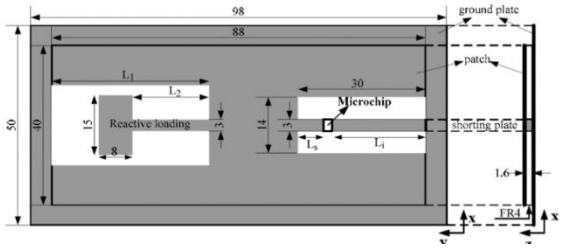

Fig. 8. Inset-feed rectangular patch with reactive load [32].

final set of the systematic review procedure and their structures are involved in cross-layered constructions such as metal vias, shorting pins or metallic plates. The inclusion of shorting elements in the structure of the designed tags increases the structure complexity and the fabrication cost. In the following subsections, the reported structures and approaches to accomplish a wideband/dual-band UHF RFID tag for metallic objects are presented.

1. Parasitic Elements

Another resonant frequency could complement the fundamental mode, which widens the tag bandwidth via the inclusion of parasitic elements in the designed structure. This addition involves a gap coupled to the driven patch. Few studies in the literature utilized parasitic element approaches to excite extra resonant frequencies to broaden the tag bandwidth [27]–[29], normally resulting in large antenna sizes. The structure described in [27] comprises feeding lines connected directly to a loop that is delimited by a slot with a width of 1 mm. In addition, two quarter-wavelength patches are grounded at the longitudinal edges by two shorting plates as shown in Figure 5(a). The loop dimensions are tuned to conjugate the impedance with a mounted IC chip over a broad frequency range, whilst adjusting the dimensions of patches and gap parameters determines the resonant frequency of the tag. In [28], the tag structure comprises a driven patch with an inset feedline shorted to the ground plane and two parasitic patches, as exhibited in Figure 5(b). The length of the parasitic patches is different from that of the driven patch. The driven patch excites the fundamental mode, whereas the two parasitic patches generate two extra resonant modes, which entails broadening the operating bandwidth. In [29], the proposed tag comprises a grooved patch, wherein asymmetric star-shaped slot is embedded, excited by the embedded L-shaped feedline with a shorted terminal using pin as shown in Figure 5(c). A relatively high gain is achieved due to the utilization of the embedded feedline. The impedance matching requirement is thus fulfilled by the embedded feed network. Two resonant modes are precisely controlled by adjusted the dimensions of the etched slots.

2. Flipping Tag

Designing a tag antenna with dual-band performance based on flipping the tag on a metallic structure, is an attractive approach. The concept is simple and allow tag operation in Lower European or North American bands. The operating band of the tag determines which side of the tag faces the metal surface. In [30], the proposed structure comprises an uneven length of two parallel laminated copper planes on the upper and lower side of the tag, wherein eight metal vias shorted the structure and lengthened the current path as shown in Figure 6. The main parameters controlling the resonant frequency include the overall length and the metal vias position. Flipping the tag on the metal surface allows the tags to interact differently based on which side faces the metallic objects. Consequently, the tag offers dual-band behavior. The aforementioned structure has been integrated with the temperature sensor, making the tag an ideal candidate for sensing applications. However, the structure thickness exceeds 2 mm, which makes it unsuitable for certain

applications. The substrate possesses a high-dielectric constant, which increases the cost of the tag. In addition, implementing the presented idea to ensure seamless operations in different countries is difficult.

3. Two-Patch Arrays

The Monza 4 IC chip possesses dual antenna ports, enabling antenna design diversity. This may lead to designs that diminish the orientation sensitivity of the tag. Furthermore, this type of IC chip can improve the reading distance and the writing range. The two antennas could interact with Monza 4 IC chip through its differential ports, where each antenna operates independently as shown in Figure 7(a). The received power in the form of electromagnetic field is induced in the pair, and demodulator gathers and processes both antenna signals on-chip [58]. In [31], two patch arrays have a cross-connection with Monza 4 IC chip for designing dual-band structures, as shown in Figure 7(b). The excited resonant frequencies are controlled by adjusting the length of patches, whilst the differences between two bands are tuned by adjusting the patch widths. At the end of the substrate, the two patch arrays are shorted to the ground plane. As a result, the tag size is miniaturized as quarter wavelength resonant antenna. The dual-port impedance is readily matched with two array patch impedances by adjusting the dimensions of the defected slots, thus forming a dual-band UHF tag antenna.

4. Reactive Load to the Main Radiating Body

Integration of the tag with a reactive load widens the tag bandwidth. This is achieved by exciting a new resonant frequency adjacent to a fundamental mode. In [32], an inset-feed rectangular patch loaded with reactive load was proposed as shown in Figure 8. The open stub was shorted to the ground plane by a metallic strip to reduce the severe effects of metal structures on the tag performance. The impedance matching between the antenna and IC chip is obtained by adjusting the inset feedline and the shorted stub. The broadband tag antenna is realized by integrating a T-shaped microstrip line into the etched slot on the radiating patch structure, which excites the second resonance, resulting in a broad impedance bandwidth covering the desired frequencies over the UHF band.

5. Adjusting/Defecting the Main Radiating Body

Designing a tag antenna with a broad bandwidth while maintaining its low profile is challenging. On the other hand, utilization of a thick substrate is a simple way to obtain wide impedance bandwidth [48]. However, this approach is impractical for certain applications. An effective way to obtain a single-layer structure is to excite multiple modes by modelling/varying the patch structure. When each mode is resonant in the vicinity of others, the tag bandwidth can be widened. Within this approach, various designs have been proposed, e.g., by etching the radiating body to form slits/slots to excite new resonant frequencies, resulting in a widened impedance bandwidth. The work presented in [33] is a single patch with two-slit structure that excites the second resonant mode close to the first mode. The inset-fed patch is grounded by the open microstrip stub, which provides an inductive reactance by varying the dimensions of the open stub. Thus, the matching with the selected IC chip can be ensured. The second resonant mode is excited due etching of two slits from the radiating edge deep into the patch center as shown in Figure 9(a). The length of slits determines the resonant frequency, where it is chosen to be slightly longer than a half-length of the patch. The antenna cross-section (*xz*-plane) is considered a perfect magnetic conductive (PMC) wall due to the symmetric structure. Hence, the total size is shrunk by splitting the antenna at the center along the *xz*-plane. Figure 9(b) presents the single-slit antenna; however, the characteristics of both antennas are similar. The tag proposed in [34] involves the inset feed patch with asymmetric slits etched from the non-radiating edge to the center as shown in Figure 9(c). The inset feeding techniques facilitate impedance matching, wherein shorting the open stub contributes to a large inductance into the input impedance [59]. Two modes can be generated by appropriately embedding two asymmetrical slits and controlling the inset feed network position.

In [35], [36], a similar structure has been presented: an inset feed rectangular patch with a pair of embedded U-shaped slots in [35], and a pair of embedded E-shaped slots in [36] as shown in Figures 9(d) and 9(e), respectively. The inset feedlines split into grounded stub by a via-hole and the inset-feed line. In [35], the embedding of U-shaped slots excited a new resonant mode close to the fundamental mode. The matching with an IC chip over resonant frequencies for both modes could be achieved by modifying the inset length and the distance between the shorting element and the IC chip for the first mode. Variations in the length, width, and location of the arm of U-shaped slots from the patch edge were utilized to match impedance with the IC chip for the second mode. In [36], the embedding of the E-shaped slots excited new resonant frequency, whilst slot dimensions forming broadband characteristics were adjusted by moving both resonant frequencies close to each other. The impedance matching is accomplished by adjusting the inset length that controls the real part of antenna impedance and the length between the IC chip and shorted element, which effectively modified the reactive part of the antenna impedance.

The work presented in [37] is a tag with orthogonal polarizations, where the linear-polarization at the Lower European band is orthogonal to polarization at the North American band. The proposed tag is designed on a 3-mm-thick substrate with high dielectric constant of 40 for miniaturization purpose. The tag structure comprises inset feed patch antenna, where the inset feed part is shorted to the ground plane using a vertical strip. The designed tag exhibits orthogonal polarization and a dual-band operation due to modifications implemented on the radiating patch. The patch is extended to the vertical side of the dielectric slab and a narrow slit is etched at the edge of the radiating patch. Thus, a part of vertical extension is removed as shown in Figure 9(f). The dual-band operation is achieved due to the embedding a narrow slit and shifting up both resonant frequencies because of the removed portion of the vertical extension. Notably, the impedance bandwidth could be

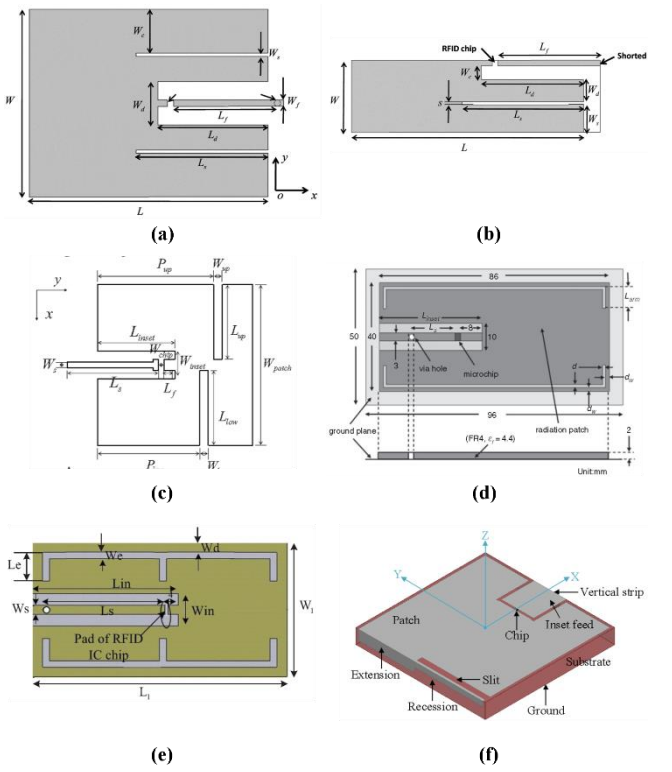

Fig. 9.(a) Inset feed patch with a two-slit structure [33] **(b)** single-slit antenna [33] **(c)** inset feed patch with asymmetric slits [34] **(d)** inset feed rectangular patch with a pair of embedded U-shaped slots [35] **(e)** inset feed rectangular patch with a pair of embedded E-shaped slots [36] **(f)** a tag with orthogonal polarizations [37].

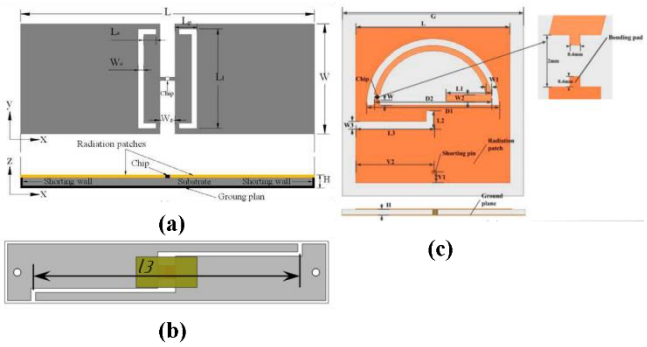

Fig. 10.(a) Two rectangular patches and loaded with shorting walls and a pair of U-shaped slots embedded on radiating patches [38] **(b)** a microstrip loop antenna with two symmetrical slots [39] **(c)** a semicircle-shaped slot etched inside a square patch embedded with a bent feedline [40].

improved by embedding suitable slots/slits in the radiating structure, which would degrade the tag radiation efficiency and gain, affecting the detection distance [35].

6. Model Matching Mode

The IC chip possesses a capacitive reactance that should be matched with the inductive reactance of the antenna. This condition indicates that a maximum power transmission coefficient can be accomplished when an ideal impedance matching is observed over the resonant frequencies. The modification of antenna structure, such as embedding a slot or a slit, is an approach to design a tag antenna with broad operations by facilitating antenna impedance compliance with the varied value of the IC chip impedance over a wide range of frequencies, thus showing a prominent performance. The structure reported in [42] comprises two rectangular patches grounded by shorting walls from their edges. A pair of symmetric U-shaped slots are embedded in both patches to expand the tag bandwidth and make it compact. The structure is shown in Figure 10(a). The impedance matching is achieved by adjusting the geometry parameters of the slots. Notably, this design features a flexible structure, where its fabrication material is PET substrate to facilitate mounting on bended surfaces. In [43], a microstrip loop antenna containing shorting elements (via holes) and two slots as shunt capacitance is embedded to match the input impedance of the IC chip as shown in Figure 10(b). The inductive reactance of antenna increases with the slot length and its thickness is 3.2 mm, which is not preferable to be mounted on metal surfaces. The structure suggested in [44] comprising a square patch is defected with a semicircle-shaped slot, where a feedline is embedded inside the etched slot. The feedline is bent to form a semi-annular-shaped feedline for exciting the radiating patch. The antenna size is reduced and its 3-dB axial ratio bandwidth is improved by etching an L-shaped slot as shown in Figure 10(c). The deterioration in the tag performance can be mitigated when the tag mounted onto the metal structures utilizes shorting pins. The impedance matching can be easily adjusted by lengthening the semi-annular feedline and coupling distance with the radiating patch. This approach entails an excellent match with the IC chip impedance over a wide range of operating frequencies.

7. Multi-Branch Structure

A broad bandwidth can be obtained by exciting different resonant frequencies using multi-branch structures. The work proposed in [41] comprise four microstrip lines with a modified meandered shape and small rectangular patch grounded using a metallic plate, as shown in Figure 11(a). The microstrip feeding line is embedded amongst three meandered lines, whereas the input impedance can be adjusted by changing the length of the feeding line. The structure excites three resonant frequencies that cover the Lower European, North American and Japan (its adopted frequency range has been changed to be a part of the North American band) bands. The shorting element increases the immunity of the tag when placed onto a metallic structure that works as a reflector and improves the radiation properties of tag antennas. In [42], the structure comprises dual-PIFA element for covering two UHF bands (Lower European and North American bands) and surrounded by coil of six loops for high-frequency band, as shown in Figure 11(b). The structure excites dual-resonance frequencies that operate over desired frequency ranges.

C. Air Gap or Foam Separation between Ground Plane and Printed Antenna Substrate:

A proper design of an RFID tag plays a major role in the RFID system and is desired to perform well whilst mounted onto metal structures. This review presents different design approaches to reduce the effect of the metallic objects on the tag performance in terms of bandwidth, input impedance, and

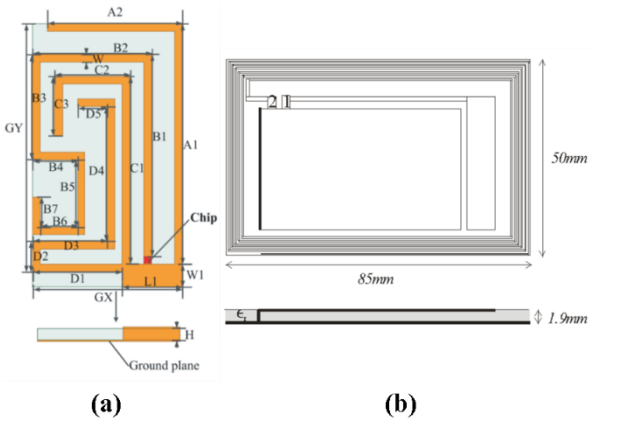

Fig. 11. (a) Four dipoles with different meandered shapes [41] **(b)** tag antenna of dual PIFA element and coil of six rounds [42].

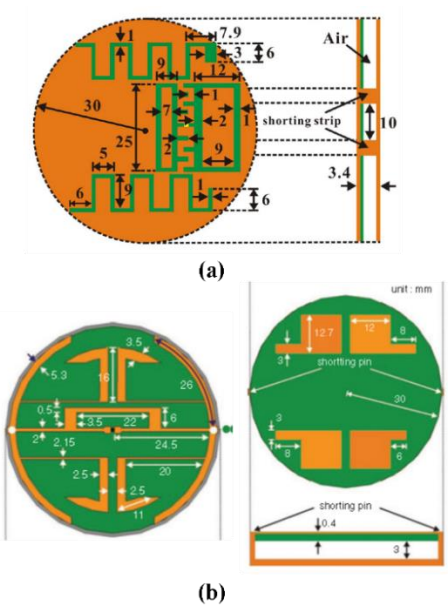

Fig. 12. (a) A circular tag antenna with meandered slits and parasitic strips [43] **(b)** dipole antenna loaded with L-shaped and parasitic step strips printed on the backside of the antenna [44].

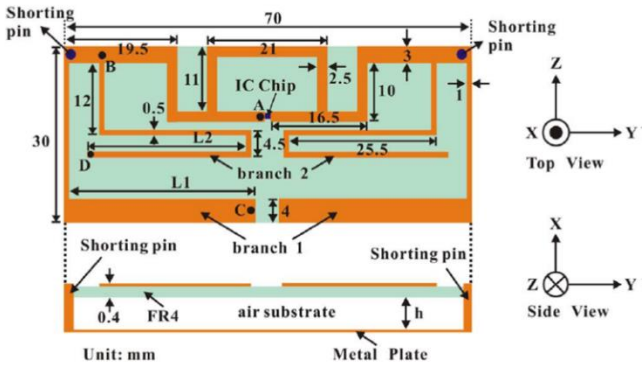

Fig. 13. Dual-branch dipole strips antenna with shorting pins posted at the antenna corner [45].

radiation efficiency. The immunity of the tag antenna to the metallic surface could be boosted by the inclusion of a shorting element to the ground layer. Further reinforcement is realized by inserting an air gap or foam layer between the printed antenna substrate and the ground layer. This structure improves the current distribution on the radiating structure and confines there in rather than the ground plane. Furthermore, this approach improves the operating bandwidth and the radiation efficiency because the effective dielectric constant value is reduced. In the following we briefly outline the works describing tag antennas designed using the aforementioned or similar methodologies.

1. Defect or Load the Main Radiating Body and Embedding Parasitic Elements

This approach depends on defecting/adjusting the radiating structure and embedding parasitic elements to achieve the targeted bandwidth. A circular RFID tag with dual-meandered slits has been proposed in [43]. The structure comprises meandered strips with mounted IC chip, dual-parasitic strips near the IC chip, and asymmetrical dual-meandered slits with different geometries at the slit end. The proposed structure excites dual-resonance frequencies close to each other, which improves the operating bandwidth. Further improvement has been reported by introducing parasitic strips near the IC chip as shown in Figure 12(a). The structure includes an air gap between the substrate and the ground layer. The circular RFID tag and parasitic step strips are presented in [44]. Dual T-arc-shaped strips connected directly to the IC chip are also connected using an inverted U-shaped shunt stub. Two shorting pins are positioned at the T-junction connecting to the ground layer, reducing the metallic structure effect. Two pairs of L-shaped strips are loaded to T-arc-shaped dipole and parasitic step strips are placed on the back side of the antenna, improving its operating bandwidth. An air gap is introduced between substrate and ground plane as shown in Figure 12(b).

2. Dual-Branch Structure

An additional resonant frequency can be introduced to broaden the tag bandwidth by embedding a branch strip and properly adjusting its dimension. A dual-branch dipole strips antenna is introduced in [45]. The proposed antenna is designed with shorting pins posted at the antenna corner, and a shunt stub (inverted U-shaped stub) formed a close loop around the feeding points as shown in Figure 13. The second branch strip excites a new resonant frequency near the main mode. Thus, the proper design of dual-branch dipole antenna and posting shorting pins lead to two resonant frequencies that are coherently excited. In this design, the ideal impedance matching with mounted IC chip is obtained due to the embedded U-shaped shunt stub. A broadband performance is accomplished whilst the tag is mounted on a metallic surface.

3. Model Matching Mode

Implementing a tag antenna on metal environments is possible, but maintaining its wide operation becomes problematic. The impedance matching mode is an effective approach to achieve wide operation over the desired range, wherein antenna impedance is consistent with the varying IC chip impedance. The design tag in [46] achieved impedance matching over two different adopted frequency ranges. A

transmission line loaded with a resonator, which is located between the slotted patch and the microchip, is utilized as dual-band impedance matching mode, as shown in Figure 14(a). The split ring resonator (SRR) is applied to accomplish the impedance requirements; SRR can be modeled as *LC* resonant tank. The coupling distance between the transmission line and *SRR* affected the distance between both resonant frequencies: strong coupling results in increasing the space between both resonant frequencies, whereas weak coupling creates a small split-off between the frequencies.

The works reported in [47], [48] indicate the insertion of a foam layer between the antenna and the ground plane. Both structures comprise a feeding loop and two radiating patches shorted to the ground by shorting strips as shown in Figures 14(b) and 14(c), respectively. In [48], the input impedance can be tuned by adjusting the T-matching network and the distance between patches, wherein wide bandwidth can be attained due to the impedance matching with the IC chip. In [47], the feeding loop and two open stubs are adjusted to obtain an excellent impedance matching. The effect of the metal structure is reduced by incorporating two shorting strips. The tag bandwidth can be tuned by the width of shorting strips and the distance between the two patches.

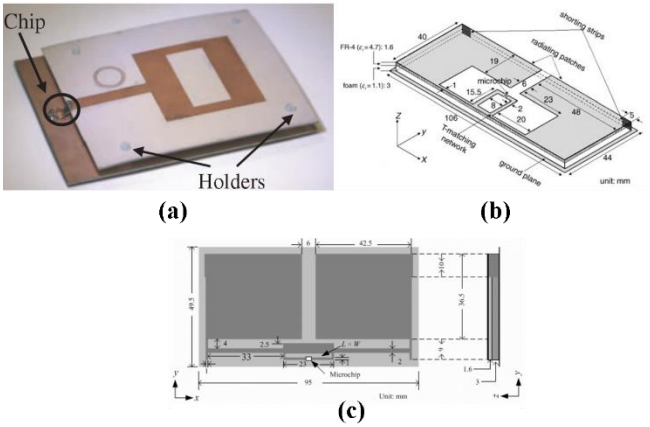

Fig. 14. (a) Slotted patch and impedance matching network [46] **(b)** RFID tag with T-matching network and two shorted radiating patches by shorting strips [47] **(c)** tag antenna with feeding loop and two symmetrical radiating patches grounded by two shoring strips [48].

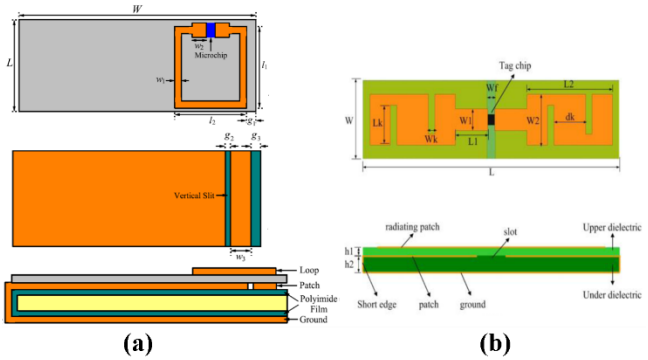

Fig. 15. (a) Rectangular feeding loop positioned on the top side of the upper layer and the underneath layer is wrapped with laminated one-side polyimide film [49] **(b)** dipole-type patch with four slits on the upper substrate and wrapped the second layer with metal strap etched with vertical slit [50].

D. Dual-Layer Tag Antenna

A traditional approach to design broadband tag antennas is to utilize parasitic elements coplanar with the main patch or stacked on the main patch, which generates numerous neighboring resonant frequencies, consequently widening the operating bandwidth [11], [60]–[63]. In addition, the capacitive coupling approach can be utilized to design a broadband tag antenna [64]. However, practical implementation of these approaches results in bulky structures, which increases the fabrication process complexity and the fabrication cost, thus limiting their applicability. Thus, utilizing the available size as much as possible, wherein the performance of the tag is proportional to the electrical size of antenna, is necessary [65]. Utilization of the parasitic elements positioned between the radiating patch and the ground layer could improve the performance of the RFID tag in terms of bandwidth, radiation efficiency, and gain [66]. The reported works demonstrating a construction of dual dielectric substrates are exhibited herein and the employed approaches to widen the bandwidth are explained. These works feature thick structures of more than 2 mm, which is not preferable to be mounted onto objects.

1. Parasitic Elements and Achieved Model Matching Mode

The tag antenna operates efficiently when a conjugate matching is obtained with the IC chip. The immunity of RFID tags increases by wrapping the underneath substrate with a metal strap. The structures presented in this sub-subsection are constructed based on dual-layered structures and achieve wide bandwidths using the model matching mode.

The works reported in [49], [50] presented a broadband UHF tag that features a dual-layer structure. The radiating body is located on the upper substrate, whereas the metallic strap is folded around the underneath layer with a slit on its upper side. In [49], a tag antenna is designed using a proximity-coupled feed approach, which comprises a rectangular feeding loop positioned on the top side of the upper layer (substrate 1), and the underneath layer (substrate 2) wrapped with laminated one-side polyimide film; further, a dual-side adhesive is used to fix the fabricated film, as shown in Figure 15(a). It forms the patch, a shorting wall and a ground plane of substrate 2. The structure of the tag is completed by stacking the upper layer above the wrapped substrate. The conjugate match with the IC chip is accomplished by introducing vertical slits into the design, which improves the impedance matching and widens the tag operating bandwidth significantly. It is possible to tune the bandwidth by varying the width and the position of the slit without changing the tag size. In [50], the structure of the tag includes two substrates, wherein the dipole-type-patch is designed with four slits on the top of upper dielectric substrate (substrate 1). The underneath substrate (substrate 2) is wrapped with a metal strap and a vertical slit is positioned on its upper side, as shown in Figure 15(b). The antenna impedance can be varied by adjusting the dimension of dipole-type-patch and four slits and the position and dimensions of vertical slit on the upper side of substrate 2. Therefore, a wide tag performance is obtained.

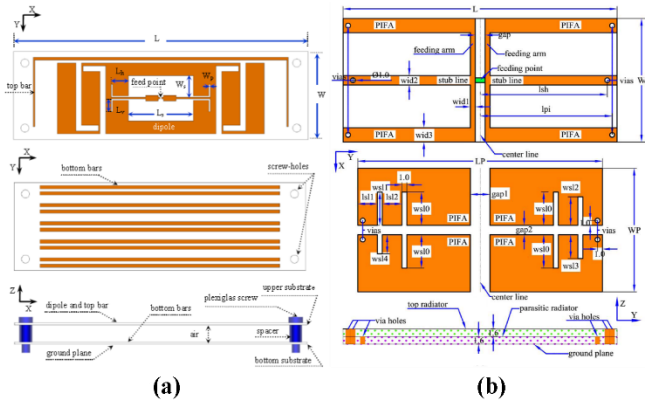

Fig. 16. (a) Tag antenna with modified dipole, mender bar, and parasitic bars [51] **(b)** tag antenna comprises four slim PIFAs on the upper side of upper substrate and four parasitic PIFAs printed on the top of the second layer [52].

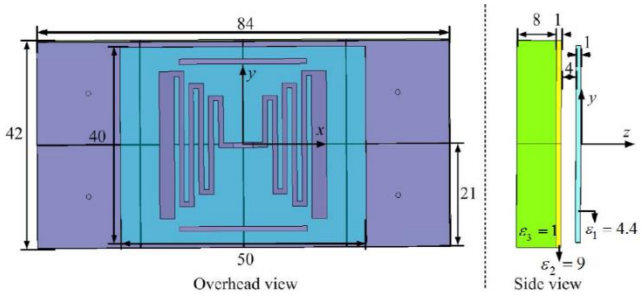

Fig. 17. Tag antenna comprises folded dipole AMC configuration [53].

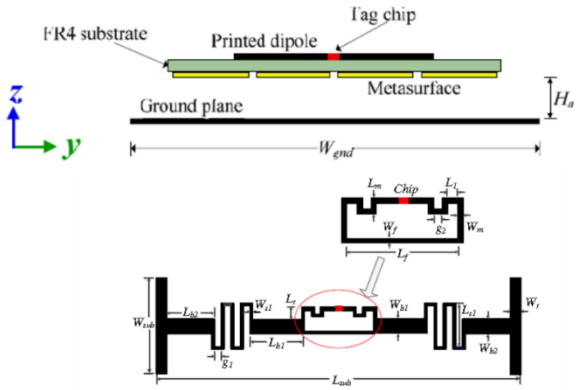

Fig. 18. Side view of tag antenna with the metasurface structure and the printed modified dipole [54].

2. Parasitic Elements and Excited Different Resonant Frequencies

A tag antenna with embedded parasitic elements possesses the capability to create new resonant frequencies close to each other that broaden the tag operating bandwidth over a specific range. This structure is an introduced approach in the literature to design tag antenna with wide operations.

The tag proposed in [51] is constructed as a dual-layer structure with the layers separated using the air gap to improve the tag gain. A meander bar and a modified dipole are placed on the top face of the upper layer. Two slits are embedded on each end of the dipole for size reduction as shown in Figure 16(a). In addition, the feedline length is extended by embedding two symmetrical slits in the center directly adjacent to the feedlines to increase the antenna inductance and to obtain impedance matching with the IC chip. The input impedance can be easily and precisely adjusted by modifying the feed lines and the center slits. Parallel bars are also introduced on the upper face of the second substrate, creating multi-resonant frequencies in the desired frequency range. Four plastic screws are positioned at the corners of each substrate to maintain fixed distance separation of the dual-layer structure. The proposed RFID tag introduces four resonant frequencies, wherein the first resonant is excited due to the meander bar, whereas the second resonant mode is generated by the modified dipole. The third and the fourth resonant modes occurred due to the printed bars on the top of the second substrate. Each resonant frequency can be adjusted easily, and the different regions of the RFID band are covered by varying the lengths. The structure suggested in [52] comprises a dual-layer construction, which shows four slim PIFAs and two shorted stub lines. The through-hole via positioned at the end of each stub lines helped achieving input impedance matching with the IC chip. A parasitic four planar PIFAs on top of the second substrate are embedded to excite four resonant frequencies simultaneously and to widen the tag bandwidth, as shown in Figure 16(b). The impedance matching for four resonant frequencies is obtained by adjusting the embedded slits in each parasitic planar PIFA.

E. Using AMC Substrate

One of the approaches introduced in the literature to design of broadband UHF tags is the use of an AMC substrate. The artificial magnetic conductor (AMC) is a surface which can improve the antenna gain due to in-phase reflection properties. The AMC substrate with a wide range of operation frequencies can cover the tag bandwidth; thus, maintaining the wideband operation of RFID tags is essential. The AMC layer as an approach to design wideband tag antennas and to increase the immunity of RFID tags to metallic structure effects. In addition, the suggested approach allows direct placement of the RFID tag on metal or dielectric materials with a high dielectric constant without performance degradation.

The work reported in [53] comprises a folded dipole AMC construction. Two bars are placed near the radiating dipole to increase the antenna inductance to achieve impedance matching with the IC chip. The distance between radiating elements and the AMC substrate is 4 mm (air gap). In addition, the distance between the AMC substrate and metallic ground is 8 mm and foam filled this gap, as shown in Figure 17. Shorting vias are involved in the structure of AMC substrate connecting unit cells to the ground plane. The broadband operation of the AMC substrate allows the coverage capability of the tag bandwidth, resulting in a wideband operation of the entire structure.

The structure proposed in [54] incorporated a modified dipole with the T-matching network and a metasurface on the top and the bottom faces of the substrate, respectively, as shown in Figure 18. Hence, this approach mimics a perfect magnetic conductor over certain frequencies. The metasurface works as an AMC layer between the designed antenna and the reflector, forming low-profile structure and unidirectional radiation. Furthermore, the second resonant frequency is excited due to the metasurface structure, which resulted in a dual-band UHF

RFID tag antenna. The conjugate match with the IC chip is obtained by adjusted the T-matching network. The designed structure is stacked over a metallic reflector and an air gap as a spacer. Compact size is achieved by enlarging of the ends of the modified dipole end.

V. Bandwidth Segmentation for IoT Applications

RFID is an attractive technology for the proliferation of IoT and industry 4.0 implementations [68], [69]. RFID technology is employed to identify and detect objects in proximity because it is efficient, durable, and cost-effective [1]. Broadband/dual-band UHF RFID tag antennas can extend the use of RFID technology in IoT applications by segmenting the operation bandwidth into two segments that comply with the most adopted frequency ranges (Lower European and North American bands). The UHF RFID readers received the backscattered ID from the RFID tag along with the signal's RSSI (received signal strength indication) and the frequency where this received value of RSSI has been reported. Each bandwidth segment is appointed to a particular zone/area. Identifying the maximum RSSI of signal in which bandwidth segment is observed, will hence indicate the location of the tagged object.

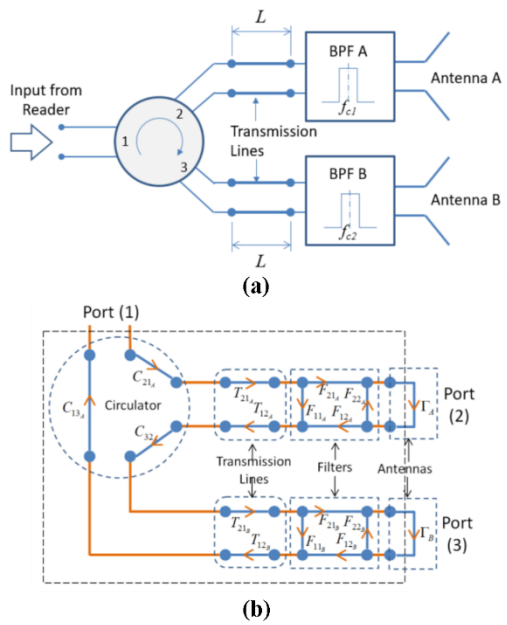

Fig. 19. Bandwidth segmentation technique [67] **(a)** the layout employing two band-pass filters and circulator (b) signal flow of two bandwidth segments.

In [67] a technique has been suggested to split the RFID bandwidth into two smaller segments to support of the utilization of UHF RFID system in IoT applications. The UHF RFID frequency range is separated between two antennas (A&B) by the use of two band-pass filters (F_A&F_B) allocated at the Lower European and North American bands where the reader can only operate (either receive or send). The layout of this technique, employing two band-pass filters and one circulator, has been shown in Fig. 19(a). The first filter F_A covers the Lower European band, whereas the second filter F_B involves the North American band. The signal flow of the proposed layout has been presented in Fig. 19(b). The operating principle is that the transmitted power will be passed to the antenna if comply with the band-pass filter otherwise it will be circulated to the following antenna. In general, *N*-1 cascaded circulators are required to achieve *N* bandwidth segments. The value of signal's RSSI is determine where tag located either in front or back of the antenna (A&B). Accordingly, the position of RFID tags can be indicated by determining the frequency of the highest RSSI value, which either fall in the segment A or segment B. An important feature of this approach is that the RFID reader is able to cover both areas instead of covering only the signal area. Furthermore, the broadband/dual-band UHF RFID tag antennas exhibit the ability to extend the implementations of aforementioned approach into IoT domain.

VI. Recommendations and Future Directions

Passive UHF RFID systems are mature ecosystems, yet experiencing a high growth rate wherever passive RFID tags are dominant in the large segment of the market. Its future is promising [70]. Employing the RFID technology in the retail sector aims to improve inventory visibility and to decrease the expense of the operation. In addition, adopting RFID technology in numerous sectors, such as healthcare, automotive, transportation, structure engineering and asset tracking, showed notable development and expansion of its use [71]–[74]. Passive tag applications are currently widespread in modern wireless technologies, such as sensor networks and the IoT. Thus, potential implementations of RFID technology due to the evolution of the RFID software, tags types, and readers must be persistently developed [75]–[77]. However, the new implementations always encounter challenges, whereas scholars and engineers explore new approaches to find a solution and improve the existing technology. To keep follow the continuous growth of the RFID technology, the governments should define suitable regulations, whereas the researchers should remain motivated to design tags that are compatible with the proposed applications.

A. Governments

The standards of support policymakers include international trade improvement, the constant growth of the technology and expense reduction. The emergence and development of the RFID technology required standards to reflect the importance of this technology in reality. Thus, the current study attempts to define how RFID systems could be used seamlessly worldwide. This step required consensus from the technical committee in each country to improve the quality of the service. Based on the report published by GS1 in Feb 2022 [14], only 81 countries define their regulation considering allocated frequencies and allowed radiated power, whilst other countries currently do not adopt these regulations. Notably, 32 countries adopted a frequency range in the North American band whilst 3 0 countries allocated a frequency range in the Lower European band. However, 1 5countries allocated frequency ranges in both the Lower European and North American bands. Whereas,

adopting similar regulations across different countries can reduce operation costs, as well as support utilization of the RFID technology.

B. Researchers

The scope of this study is an overview of design techniques for broadband/dual-band UHF RFID tags implementable on metallic structures. Initially, the designed tag must be compatible with the regulations of the country in terms of the allocated frequency range. In addition, the bandwidth of the tag should fulfil the defined criterion, which is 3-dB *RL* bandwidth. Furthermore, antenna engineers should take have in mind a number of prerequisites during the design process. The design procedure starts by choosing a suitable and inexpensive substrate that plays a crucial role in performance estimation: a high permittivity substrate is used for achieving size reduction, whereas low permittivity substrate is employed to design broadband RFID tags [34], [78]. Another consideration is the antenna size and structure. The tag size should not exceed 2500 mm^2 to be suitable for tagging small-scale items. At this level, the antenna should be a miniature single-layer structure without cross-layered constructions that does not require a complex fabrication procedure. These features decrement the tag cost, increasing its suitability for mass production. Attaching products regardless of their size or shape can be realized without difficulty due to the miniature size of RFID tags. The large footprint of the tag increases detection probability and system reliability. However, maintaining the tag performance while reducing its size is a challenging endeavor. Further, the tag must be compatible with the attached objects. On the other hand, utilizing the tag in an environment involving conductive objects is problematic [79]–[82]. The designed structure must increase the immunity of the RFID tag to the proximity of metal surfaces and preferably enable attachment to different dielectric substrates. The tag performance is critical for the success or failure of RFID systems. Consequently, the principles of designing tag antenna must be well-known by RFID tag designers. These principles consider the sensitivity of the IC chip, impedance matching, backscattering performance, operating frequency range, size and shape of the tagged surface and surrounding environment [83]. The following considerations are of importance:

- Designed tag covers a desired frequency range (bandwidth requirement).
- The performance of the tag is acceptable over operating frequencies wherein its reading distance meets the system requirements.
- The occupied size is small and designed on a single layer without cross-layered construction.
- The structure can perform well whilst attached onto metallic surfaces or dielectric substrates regardless of their size and shape.

VII. Conclusion

The key contribution of this study is a comprehensive review and classification of the gathered literature works based on the tag structure and the employed approaches to bandwidth enhancement. The RFID tags, which can operate over a wide range of frequencies, are suitable to work seamlessly across different countries. The final choice of the articles outlines in this paper was dictated by the designed query in three scientific engines, as elaborated on in the methodology section. The selected articles were assessed by their reported specifications, such as achieved bandwidth requirement, tag performance, occupied size, tag construction, and compatibility with metallic surfaces regardless of their size and shape. The design standards of wideband/dual-band metal-mountable tags play a vital role in expanding the use of RFID technology in a globalized economy. Governments should define compatible regulations, whereas researchers should design tag structures that meets specifications concerning compact size, single-layer structure (without cross-layered constructions), and straightforward fabrication procedure. This presentation gives a perspective and, hopefully, contributes to increased understanding of the addressed topic for future endeavors.

References

[1] B. S. Çiftler, A. Kadri, and I. Güvenç, "IoT localization for bistatic passive UHF RFID systems with 3-D radiation pattern," *IEEE Internet Things J.*, vol. 4, no. 4, pp. 905–916, 2017, doi: 10.1109/JIOT.2017.2699976.

[2] X. Zhang, H. X. Li, and H. S. H. Chung, "Setup-independent sensing architecture with multiple UHF RFID sensor tags," *IEEE Internet Things J.*, vol. 9, no. 2, pp. 1243–1251, 2022, doi: 10.1109/JIOT.2021.3079448.

[3] S. Y. Ooi, P. S. Chee, E. H. Lim, Y. H. Lee, and F. L. Bong, "Stacked planar inverted-L antenna with enhanced capacitance for compact tag design," *IEEE Trans. Antennas Propag.*, vol. 70, no. 3, pp. 1816–1823, 2022, doi: 10.1109/TAP.2021.3118822.

[4] S. M. Chiang, E. H. Lim, P. S. Chee, Y. H. Lee, and F. L. Bong, "Dipolar tag antenna with a top-loading inductive channel with broad range frequency tuning capability," *IEEE Trans. Antennas Propag.*, vol. 70, no. 3, pp. 1653–1662, 2022, doi: 10.1109/TAP.2021.3111093.

[5] K. N. Salman, A. Ismail, R. S. A. Raja Abdullah, and T. Saeedi, "Coplanar UHF RFID tag antenna with U-shaped inductively coupled feed for metallic applications," *PLoS One*, vol. 12, no. 6, p. e0178388, Jun. 2017, doi: 10.1371/journal.pone.0178388.

[6] F. Erman *et al.*, "Low-profile folded dipole UHF RFID tag antenna with outer strip lines for metal mounting application," *Turkish J. Electr. Eng. Comput. Sci.*, vol. 28, pp. 2643–2656, 2020, doi: 10.3906/elk-1912-45.

[7] K. Mohammadpour-Aghdam, S. Radiom, R. Faraji-Dana, G. A. Vandenbosch, and G. G. Gielen, "Miniaturized RFID/UWB antenna structure that can be optimized for arbitrary input impedance," *IEEE Antennas Propag. Mag.*, vol. 54, no. 2, pp. 74–87, 2012, doi: 10.1109/MAP.2012.6230719.

[8] E. Perret, S. Tedjini, and R. S. Nair, "Design of antennas for UHF RFID tags," *Proc. IEEE*, vol. 100, no. 7, pp. 2330–2340, 2012, doi: 10.1109/JPROC.2012.2186950.

[9] R. Abdulghafor *et al.*, "Recent advances in passive UHF-RFID tag antenna design for improved read range in product packaging applications: a oomprehensive review," *IEEE Access*, vol. 9, pp. 63611–63635, 2021, doi: 10.1109/ACCESS.2021.3074339.

[10] F. Erman *et al.*, "Low-profile interdigitated UHF RFID tag antenna for metallic objects," *IEEE Access*, vol. 10, pp. 90915–90923, 2022, doi: 10.1109/access.2022.3201644.

[11] H. W. Son and S. H. Jeong, "Wideband RFID tag antenna for metallic surfaces using proximity-coupled feed," *IEEE Antennas Wirel. Propag. Lett.*, vol. 10, pp. 377–380, 2011, doi: 10.1109/LAWP.2011.2148151.

[12] M. J. Page *et al.*, "PRISMA 2020 explanation and elaboration: Updated guidance and exemplars for reporting systematic reviews," *BMJ*, vol. 372, 2021, doi: 10.1136/bmj.n160.

[13] "What is GS1 ? An overview," 2008. Accessed: Sep. 11, 2022. [Online]. Available: https://www.gs1.org/sites/default/files/docs/what_is_gs1.pdf.

[14] "Overview of UHF frequency allocations (860 to 960 MHz) for RAIN RFID," 2022. Accessed: Jul. 15, 2022. [Online]. Available: https://www.gs1.org/sites/default/files/docs/epc/uhf_regulations.pdf.

[15]K. Kurokawa, "Power waves and scattering matrix," *IEEE Trans. Microw. Theory Tech.*, vol. 13, no. 2, pp. 194–202, 1965, doi: 10.1109/TMTT.1965.1125964.

[16]L. Ukkonen, L. Sydänheimo, and M. Kivikoski, "Effects of metallic plate size on the performance of microstrip patch-type tag antennas for passive RFID," *IEEE Antennas Wirel. Propag. Lett.*, vol. 4, pp. 410–413, 2005.

[17]Z. Zhang and X. Liu, "A low-profile planar broadband UHF RFID tag antenna for metallic objects," in *2013 Proceedings of the International Symposium on Antennas & Propagation*, 2013, pp. 5–8.

[18]D. Li, J. Li, and L. Mao, "A novel broadband RFID tag antenna mountable on metallic surface," in *2011 International Conference on Control, Automation and Systems Engineering (CASE)*, 2011, pp. 3–6, doi: 10.1109/ICCASE.2011.5997587.

[19]M. S. R. Bashri, M. Ibrahimy, and S. M. A. Motakabber, "Design of a planar wideband patch antenna for UHF RFID tag," *Microw. Opt. Technol. Lett.*, vol. 56, no. 7, pp. 1579–1584, 2014, doi: 10.1002/mop.

[20]M. S. R. Bashri, M. I. Ibrahimy, and S. M. A. Motakabber, "Design of a wideband inductively coupled loop feed patch antenna for UHF RFID tag," *Radioengineering*, vol. 24, no. 1, pp. 38–44, 2015, doi: 10.13164/re.2015.0038.

[21]F. You and Z. Jiang, "A broadband UHF RFID tag antenna design for metallic surface using module matching," *Prog. Electromagn. Res. Lett.*, vol. 95, pp. 83–90, 2021, doi: 10.2528/pierl20091702.

[22]J. H. Cho, H. W. Son, S. H. Jeong, W. K. Choi, and C. W. Park, "A flexible, wideband RFID tag antenna for metallic surfaces," in *IEEE Antennas and Propagation Society, AP-S International Symposium (Digest)*, 2012, pp. 3–4, doi: 10.1109/APS.2012.6349362.

[23]F. Kang and Y. Cheng, "A miniature RFID tag antenna mounted on metallic objects," in *2016 IEEE International Conference on Ubiquitous Wireless Broadband (ICUWB)*, 2016, pp. 1–3, doi: 10.1109/ICUWB.2016.7790587.

[24]M. S. R. Bashri, M. Ibrahimy, and S. M. A. Motakabber, "A compact wideband patch antenna for ultra high frquency RFID tag," *J. Control. Meas. Electron. Comput. Commun.*, vol. 56, no. 1, pp. 76–83, 2015, doi: 10.7305/automatika.2015.04.598.

[25]H. Bouazza, A. Lazaro, M. Bouya, and A. Hadjoudja, "A planar dual-band UHF RFID tag for metallic items," *Radioengineering*, vol. 29, no. 3, pp. 504–511, 2020, doi: 10.13164/RE.2020.0504.

[26]H. Bouazza, A. Lazaro, M. Bouya, and A. Hadjoudja, "Dual-band UHF RFID tag for metallic items," in *In 2019 IEEE-APS Topical Conference on Antennas and Propagation in Wireless Communications (APWC*, 2019, pp. 90–92, doi: 10.13164/RE.2020.0504.

[27]A. G. Santiago, J. R. Costa, and C. A. Fernandes, "Broadband UHF RFID passive tag antenna for near-body applications," *IEEE Antennas Wirel. Propag. Lett.*, vol. 12, pp. 136–139, 2013, doi: 10.1109/LAWP.2013.2243400.

[28]M. Lai and R. Li, "Broadband UHF RFID tag antenna with parasitic patches for metallic objects," *Microw. Opt. Technol. Lett.*, vol. 53, no. 7, pp. 14367–1470, 2011, doi: 10.1002/mop.26049.

[29]T. Pan, S. Zhang, and S. He, "Compact RFID tag antenna with circular polarization and embedded feed network for metallic objects," *IEEE Antennas Wirel. Propag. Lett.*, vol. 13, pp. 1271–1274, 2014, doi: 10.1109/LAWP.2014.2333365.

[30]K. Zannas, H. El Matbouly, Y. Duroc, and S. Tedjini, "A flipping UHF RFID sensor-tag for metallic environment compliant with ETSI/FCC bands," *IEEE Trans. Antennas Propag.*, vol. 69, no. 3, pp. 1283–1292, 2020, doi: 10.1109/TAP.2020.3026869.

[31]G. H. Du, T. Tang, and Y. Deng, "Dual-band metal skin UHF RFID tag antenna," *Electron. Lett.*, vol. 49, no. 14, pp. 900–901, 2013, doi: 10.1049/el.2013.1597.

[32]M. Y. Lai and R. L. Li, "A low-profile broadband RFID tag antenna for metallic objects," *2010 Int. Conf. Microw. Millim. Wave Technol.*, pp. 1891–1893, 2010, doi: 10.1109/ICMMT.2010.5524890.

[33]P. Yang, S. He, Y. Li, and L. Jiang, "Low-profile microstrip antenna with bandwidth enhancement for radio frequency identification applications," *Electromagnetics*, vol. 32, no. 4, pp. 244–253, 2012, doi: 10.1080/02726343.2012.672044.

[34]J. Z. Huang, P. H. Yang, W. C. Chew, and T. T. Ye, "A compact broadband patch antenna for universal UHF RFID tags," in *Asia Pacific Microwave Conference*, 2009, pp. 1044–1047, doi: 10.1002/mop.25560.

[35]L. Mo, H. Zhang, and H. Zhou, "Broadband UHF RFID tag antenna with a pair of U slots mountable on metallic objects," *Electron. Lett.*, vol. 44, no. 20, pp. 1173–1174, 2005, doi: 10.1049/el:20089813.

[36]Y. He and Z. Pan, "Design of UHF RFID broadband anti-metal tag antenna applied on surface of metallic objects," in *2013 IEEE Wireless Communications and Networking Conference (WCNC)*, 2013, pp. 4352–4357, doi: 10.1109/WCNC.2013.6555278.

[37]J. Xi and C. L. Mak, "A compact dual band RFID metal tag with orthogonal polarizations at ETSI and FCC bands," *2017 IEEE Int. Conf. RFID Technol. Appl.*, pp. 129–133, 2017, doi: 10.1109/RFID-TA.2017.8098867.

[38]T. Tang and G. H. Du, "A slim wideband and conformal UHF RFID tag antenna based on U-shaped slots for metallic objects," *Prog. Electromagn. Res. C*, vol. 38, pp. 141–151, 2013, doi: 10.2528/PIERC13011005.

[39]A. E. Popugaev and R. Wansch, "A small high performance metal-mountable RFID tag antenna," in *Proceedings of the Fourth European Conference on Antennas and Propagation, IEEE*, 2010, pp. 1–4.

[40]H. Liu, C. Liu, Q. Liu, Y. Lu, and S. He, "Compact broadband circularly polarized UHF RFID tag antenna for metallic mounting," *J. Electromagn. Waves Appl.*, vol. 34, no. 8, pp. 989–1001, 2020, doi: 10.1080/09205071.2020.1767702.

[41]C. Liu, H. Liu, and S. He, "Compact tri-band UHF RFID tag antenna for Monza4 chip," in *2016 Progress In Electromagnetics Research Symposium (PIERS)*, 2016, pp. 1312–1315, doi: 10.1109/PIERS.2016.7734644.

[42]M. Hirvonen *et al.*, "Multi-system, multi-band RFID antenna: Bridging the gap between HF-and UHF-based RFID applications," in *In 2008 European Conference on Wireless Technology Conference*, 2008, pp. 1767–1770.

[43]J. H. Lu, K. T. Hung, and H. W. Tian, "Broadband circular tag antenna attachable on the metallic objects," *2016 IEEE 5th Asia-Pacific Conf. Antennas Propag.*, pp. 449–450, 2016, doi: 10.1109/APCAP.2016.7843285.

[44]J. H. Lu and G. T. Zheng, "Broadband design of planar circular tag antenna for UHF RFID system," *Electron. Lett.*, vol. 52, no. 20, pp. 1654–1656, 2016, doi: 10.1049/el.2016.2110.

[45]J. H. Lu and G. T. Zheng, "Planar broadband tag antenna mounted on the metallic material for UHF RFID system," *IEEE Antennas Wirel. Propag. Lett.*, vol. 10, pp. 1405–1408, 2011, doi: 10.1109/LAWP.2011.2178997.

[46]F. Paredes, G. Zamora, S. Zuffanelli, F. J. Herraiz-Martinez, Ferran Martin, and J. Bonache, "Free-space and on-metal dual-band tag for UHF-RFID applications in Europe and USA," *Prog. Electromagn. Res.*, vol. 141, pp. 223-577–590, 2013.

[47]Q. Z. Chen and B. J. Hu, "Novel UHF RFID tag antenna with shorted stubs mountable on the metallic objects," *2008 Int. Conf. Microw. Millim. Wave Technol. Proc.*, vol. 4, pp. 1822–1824, 2008, doi: 10.1109/ICMMT.2008.4540834.

[48]L. Xu, S. J. Hu, and J. Wang, "UHF RFID tag antenna with broadband characteristic," *Electron. Lett.*, vol. 44, no. 2, pp. 79–81, 2008, doi: 10.1049/el:20083009.

[49]S. R. Lee, E. H. Lim, and S. K. A. Rahim, "Small Wideband Antenna for On-Metal UHF RFID Tag Design," *IEEE J. Radio Freq. Identif.*, vol. 6, pp. 121–127, 2022, doi: 10.1109/JRFID.2021.3134492.

[50]L. Yuan and W. Tang, "A compact broadband UHF RFID tag antenna for metallic objects," in *2017 International Applied Computational Electromagnetics Society Symposium in China (ACES)*, 2017, pp. 1–2.

[51]A. Hamani, M. C. E. Yagoub, T. P. Vuong, and R. Touhami, "A novel broadband antenna design for UHF RFID tags on metallic surface environments," *IEEE Antennas Wirel. Propag. Lett.*, vol. 16, pp. 91–94, 2017, doi: 10.1109/LAWP.2016.2557778.

[52]J. Zhang and Y. Long, "A dual-layer broadband compact UHF RFID tag antenna for platform tolerant application," *IEEE Trans. Antennas Propag.*, vol. 61, no. 9, pp. 4447–4455, 2013, doi: 10.1109/TAP.2013.2269472.

[53]X. Ding, S. Liu, K. Zhang, and Q. Wu, "A broadband anti-metal RFID tag with AMC ground," in *Proceedings of 2014 3rd Asia-Pacific Conference on Antennas and Propagation (APCAP)*, 2014, pp. 647–649, doi: 10.1109/APCAP.2014.6992578.

[54]T. N. Hien Doan, S. X. Ta, K. Van Nguyen, K. K. Nguyen, and C. Dao-Ngoc, "Low-profile, dual-band, unidirectional RFID tag antenna using metasurface," *Prog. Electromagn. Res. C*, vol. 93, pp. 131–141, 2019, doi: 10.2528/PIERC19041505.

[55]H.-W. Son and C.-S. Pyo, "Design of RFID tag antennas using an inductively coupled feed," *Electron. Lett.*, vol. 41, pp. 994–996, 2005.

[56]G. Marrocco, "The art of UHF RFID antenna design: impedance-matching and size-reduction techniques," *IEEE Antennas Propag. Mag.*, vol. 50, no. 1, pp. 66–79, 2008, doi: 10.1109/MAP.2008.4494504.

[57]C. K. Wu and K. L. Wong, "Broadband microstrip antenna with directly coupled and parasitic patches," *Microw. Opt. Technol. Lett.*, vol. 22, no. 5, pp. 348–349, 1999, doi: 10.1002/(SICI)1098-2760(19990905)22:5<348::AID-MOP16>3.0.CO;2-V.

[58]"IMPINJ MONZA ® 4 SERIES," 2022. Accessed: Aug. 28, 2022.

[Online]. Available: https://support.impinj.com/hc/en-us/articles/202756908-Monza-4-Datasheet.

[59]B. Lee and B. Yu, "Compact structure of UHF band RFID tag antenna mountable on metallic objects," *Microw. Opt. Technol. Lett.*, vol. 50, no. 1, pp. 232–234, 2008, doi: 10.1002/mop.23031.

[60]H. D. Chen and Y. H. Tsao, "Broadband capacitively coupled patch antenna for RFID tag mountable on metallic objects," *IEEE Antennas Wirel. Propag. Lett.*, vol. 9, pp. 489–492, 2010, doi: 10.1109/LAWP.2010.2050854.

[61]C. C. Chang and Y. C. Lo, "Broadband RFID tag antenna with capacitively coupled structure," *Electron. Lett.*, vol. 42, no. 23, pp. 1322–1323, 2006, doi: 10.1049/el:20062063.

[62]P. H. Yang, Y. Li, L. Jiang, W. C. Chew, and T. T. Ye, "Compact metallic RFID tag antennas with a loop-fed method," *IEEE Trans. Antennas Propag.*, vol. 59, no. 12, pp. 4454–4462, 2011, doi: 10.1109/TAP.2011.2165484.

[63]K. H. Lin, S. L. Chen, and R. Mittra, "A capacitively coupling multifeed slot antenna for metallic RFID tag design," *IEEE Antennas Wirel. Propag. Lett.*, vol. 9, pp. 447–450, 2010, doi: 10.1109/LAWP.2010.2048991.

[64]J. Z. Huang, P. H. Yang, W. C. Chew, and T. T. Ye, "A novel broadband patch antenna for universal UHF RFID tags," *Microw. Opt. Technol. Lett.*, vol. 52, no. 12, pp. 2653–2657, 2010, doi: 10.1002/mop.25560.

[65]C. M. Kruesi, R. J. Vyas, and M. M. Tentzeris, "Design and development of a novel 3-D cubic antenna for wireless sensor networks (WSNs) and RFID applications," *IEEE Trans. Antennas Propag.*, vol. 57, no. 10, pp. 3293–3299, 2009, doi: 10.1109/TAP.2009.2028672.

[66]L. Ukkonen, M. Schaffrath, D. W. Engels, L. Sydänheimo, and M. Kivikoski, "Operability of folded microstrip patch-type tag antenna in the UHF RFID bands within 865-928 MHz," *IEEE Antennas Wirel. Propag. Lett.*, vol. 5, pp. 414–417, 2006, doi: 10.1109/LAWP.2006.883085.

[67]H. F. Hammad, "New Technique for Segmenting RFID Bandwidth for IoT Applications," *IEEE J. Radio Freq. Identif.*, vol. 5, no. 4, pp. 446–450, 2021, doi: 10.1109/jrfid.2020.3034490.

[68]J. Li *et al.*, "PSOTrack: A RFID-based system for random moving objects tracking in unconstrained indoor environment," *IEEE Internet Things J.*, vol. 5, no. 6, pp. 4632–4641, 2018, doi: 10.1109/JIOT.2018.2795893.

[69]J. Lai *et al.*, "TagSort: Accurate relative localization exploring RFID phase spectrum matching for internet of things," *IEEE Internet Things J.*, vol. 7, no. 1, pp. 389–399, 2020, doi: 10.1109/JIOT.2019.2950174.

[70]"ChainLink Research : Research :State of the Passive UHF RFID Market," 2015. Accessed: Oct. 16, 2019. [Online]. Available: http://www.chainlinkresearch.com/media/docs/original/ChainLink2015_UHFPassiveRFID_Report.pdf.

[71]F. Erman, S. Koziel, E. Hanafi, R. Soboh, and S. Szczepanski, "Miniaturized metal-mountable U-shaped inductive-coupling-fed UHF RFID tag antenna with defected microstrip surface," *IEEE Access*, vol. 10, pp. 47301–47308, 2022, doi: 10.1109/ACCESS.2022.3171243.

[72]W. Yao, C. H. Chu, and Z. Li, "The adoption and implementation of RFID technologies in healthcare: a literature review," *J. Med. Syst.*, vol. 36, no. 6, pp. 3507–3525, 2012, doi: 10.1007/s10916-011-9789-8.

[73]A. J. Healey, P. Fathi, and N. C. Karmakar, "RFID sensors in medical applications," *IEEE J. Radio Freq. Identif.*, vol. 4, no. 3, pp. 212–221, 2020, doi: 10.1109/JRFID.2020.2997708.

[74]K. K. Duan and S. Y. Cao, "Emerging RFID technology in structural engineering – a review," *Structures*, vol. 28, pp. 2404–2414, 2020, doi: 10.1016/j.istruc.2020.10.036.

[75]H. Landaluce, L. Arjona, A. Perallos, F. Falcone, I. Angulo, and F. Muralter, "A review of IoT sensing applications and challenges using RFID and wireless sensor networks," *Sensors*, vol. 20, no. 9, p. 2495, 2020, doi: 10.3390/s20092495.

[76]B. S. Cook *et al.*, "RFID-based sensors for zero-power autonomous wireless sensor networks," *IEEE Sens. J.*, vol. 14, no. 8, pp. 2419–2431, 2014, doi: 10.1109/JSEN.2013.2297436.

[77]N. Khalid, R. Mirzavand, and A. K. Iyer, "A survey on battery-less RFID-based wireless sensors," *Micromachines*, vol. 12, no. 7, p. 819, 2021, doi: 10.3390/mi12070819.

[78]A. A. Babar, T. Bjorninen, V. A. Bhagavati, L. Sydanheimo, P. Kallio, and L. Ukkonen, "Small and flexible metal mountable passive UHF RFID tag on high-dielectric polymer-ceramic composite substrate," *IEEE Antennas Wirel. Propag. Lett.*, vol. 11, pp. 1319–1322, 2012, doi: 10.1109/LAWP.2012.2227291.

[79]H. Li, J. Zhu, and Y. Yu, "Compact Single-Layer RFID Tag Antenna Tolerant to Background Materials," *IEEE Access*, vol. 5, pp. 21070–21079, 2017, doi: 10.1109/ACCESS.2017.2756670.

[80]W. H. Ng, E. H. Lim, F. L. Bong, and B. K. Chung, "Compact planar inverted-S antenna with embedded tuning arm for on-metal UHF RFID tag design," *IEEE Trans. Antennas Propag.*, vol. 67, no. 6, pp. 4247–4252, 2019, doi: 10.1109/TAP.2019.2911191.

[81]K. Thirappa, E.-H. Lim, F.-L. Bong, and B.-K. Chung, "Compact folded-patch with orthogonal tuning slots for on-metal tag design," *IEEE Trans. Antennas Propag.*, vol. 67, no. 9, pp. 5833–5842, 2019, doi: 10.1109/tap.2019.2920324.

[82]N. Ripin, E. H. Lim, F. L. Bong, and B. K. Chung, "Miniature folded dipolar patch with embedded AMC for metal mountable tag design," *IEEE Trans. Antennas Propag.*, vol. 68, no. 5, pp. 3525–3533, 2020, doi: 10.1109/TAP.2020.2969814.

[83]E. B. Abdallah, A. Carle, and P. Mondon, "Analysis, design, and measurements of an ultrasmall on-metal UHF RFID tag antenna," *Microw. Opt. Technol. Lett.*, vol. 61, no. 11, pp. 2468–2476, 2019, doi: 10.1002/mop.31943.

FUAD ERMAN was born in Palestine. He received the B.Eng. degree in electronics and communications engineering from Al-Baath University, in 2013, the M.Eng.Sc. degree in communication and network engineering from the University of Putra Malaysia, in 2017, and the Ph.D. degree in electrical engineering from University of Malaya, in 2020. He is currently working with the Engineering Optimization and Modeling Center (EOMC), Department of Electrical Engineering, Reykjavik University, Iceland and with College of Telecommunications and Information Technology, Nablus University for Vocational & Technical Education, Ramallah, State of Palestine. His current research interests include RFID antennas, RFID sensors, and wearable antennas.

SLAWOMIR KOZIEL received the M.Sc. and Ph.D. degrees in electronic engineering from the Gdansk University of Technology, Poland, in 1995 and 2000, respectively, the M.Sc. degrees in theoretical physics and in mathematics, in 2000and 2002, respectively, and the Ph.D. degree in mathematics from the University of Gdansk, Poland, in 2003. He is currently a Professor with the Department of Engineering, Reykjavik University, Iceland. His research interests include CAD and modeling of microwave and antenna structures, simulation-driven design, surrogate-based optimization, space mapping, circuit theory, analog signal processing, evolutionary computation, and numerical analysis.

LEIFUR LEIFSSON received the bachelor's and master's degrees in mechanical engineering from the University of Iceland, Reykjavik, Iceland, in 1999 and 2000, respectively, and a doctoral degree in aerospace engineering from Virginia Tech, Blacksburg, VA, USA, in 2006. He is currently an Associate Professor of aerospace engineering with Purdue University, West Lafayette, IN, USA. His research focuses on computational modeling, optimization, and uncertainty quantification of engineered systems with an emphasis on methods for multifidelity modeling and machine learning. Current application areas include aerodynamic shape optimization, aerodynamic flutter, model-based nondestructive evaluation, microwave devices, and food-energy-water nexus.